

HIGGS

Hydrogen in Gas Grids

A systematic validation approach at various admixture levels into high-pressure grids

D4.4

Final report on systematic validation of testing loop

Date 21 December 2023 (M48)
Grant Number 875091
Author(s) **Virginia Madina**¹, Jorge Aragón,¹ Ekain Fernández,¹ Vanesa Gil^{2,3}, Javier Sánchez², Alberto Cerezo⁴, Cristina Rodríguez⁴

1 Tecnalia
 2 Fundación Hidrógeno Aragón
 3 ARAID
 4 Redexis

Author printed in bold is the contact person

Status Started / Draft / Consolidated / Review / Approved / **Submitted** / Accepted by the EC / Rework [use bold style for current state]

Dissemination level:

PU Public

RE Restricted to a group specified by the consortium*

PP Restricted to other programme participants*

CO Confidential, only for members of the consortium*

*(including the Commission Services)



This project has received funding from the Fuel Cells and Hydrogen 2 Joint Undertaking (now Clean Hydrogen Partnership) under Grant Agreement No. 875091 'HIGGS'. This Joint Undertaking receives support from the European Union's Horizon 2020 Research and Innovation program, Hydrogen Europe and Hydrogen Europe Research.

Document history

Version	Date	Description
1.1	2023-12-11	First draft
1.2	2023-12-14	Second draft
1.3	2023-12-18	Input from partners
2.0	2023-12-21	Consolidated version ready for last review
3.0	2023-12-26	Version ready for submission

The contents of this document are provided “AS IS”. It reflects only the authors’ view and the JU is not responsible for any use that may be made of the information it contains.

Table of Contents

Document history	2
Acronyms and abbreviations	7
Executive Summary	8
1 Objectives	11
2 Introduction	12
3 Test methods for the testing platform at FHa	13
3.1 Gas tightness tests	13
3.2 Gas separation test.....	14
3.3 Inspection of valves and equipment after H ₂ exposure	16
3.4 Hydrogen embrittlement tests	17
3.4.1 Constant displacement tests at FHA	18
3.4.2 Hydrogen exposure of welded API 5L	20
3.4.3 Slow Strain Rate Tests.....	21
4 Results from the experimental campaign	23
4.1 Gas tightness tests	23
4.1.1 Testing Campaign #1: 20 mol%H ₂ /80 mol% CH ₄	23
4.1.2 Testing Campaign #2: 20 mol%H ₂ /4mol%CO ₂ /11ppmv H ₂ S/76 mol% CH ₄	24
4.1.3 Testing Campaign #3: 30 mol%H ₂ /4mol%CO ₂ /11ppmv H ₂ S/66 mol% CH ₄	25
4.1.4 Testing Campaign #4: 100 mol%H ₂	25
4.2 Gas separation performance of the membrane prototype	27
4.3 Results of equipment from the dynamic section	29

4.4	Inspection of valves from the static section	33
4.4.1	Ball valve analysis (2 nd campaign).....	35
4.5	API 5L steel specimens constant displacement tests	37
4.5.1	C-ring specimens	38
4.5.2	Welded pipe sections of API 5L pipes	44
5	Slow Strain Rate Tests	46
6	Conclusions	50
	Bibliography and References.....	52
	Acknowledgements	53

List of Figures

Figure 1.	Picture of HIGGS experimental platform at Aragon Hydrogen Foundation (FHa, Spain)	13
Figure 2.	Picture of the valves testing section	14
Figure 3.	Gas separation prototype	15
Figure 4.	Picture of the testing equipment in the dynamic section	16
Figure 5.	Detail of sections of the API 5L X70 steel pipes upon reception in Tecnia	17
Figure 6.	Optical micrograph showing detail of cross section of GTA welded joint in X70 steel (left) and micro-hardness evolution in this welded joint (right)	18
Figure 7.	Picture of the pig trap (up) and the constant strain specimens allocated inside it (down)	18
Figure 8.	Welded pipe sections of the API 5L steel pipes.....	20
Figure 9.	SSRT, fracture toughness and fatigue machine for testing in H ₂ gas (left). Detail of fractured notched specimen (right).....	21
Figure 10.	Evolution of the pressure (left), and H ₂ gas composition (right) in each line of the static section during the 1 st experimental campaign (20 mol% H ₂).....	23
Figure 11.	Evolution of the pressure P/Z·T quotient (left) and H ₂ gas composition in each line of the static section during the 2 nd experimental campaign (20 mol% H ₂ + impurities of H ₂ S and CO ₂) ...	24
Figure 12.	Evolution of the pressure P/Z·T quotient (left) and H ₂ gas composition in each line of the static section during the 3 rd experimental campaign (30 mol% H ₂ + impurities of H ₂ S and CO ₂).....	25
Figure 13.	Evolution of the pressure P/Z·T in each line of the static section during the 4 th experimental campaign (100 mol% H ₂)	26
Figure 14.	Pressure against time during the internal tightness test at ΔP=70 bar (left) and ΔP=40 bar (right)	27
Figure 15.	Gas separation performance of the prototype with Membrane #1. Blue line stands for the total permeate flow and orange scatter stands for the H ₂ purity in the permeate stream	28
Figure 16.	Pressure regulator and details of blistering in valve seat at the conclusion of the 3 rd experimental campaign	30

Figure 17. Valve seats tested at 20% H_2 + impurities of CO_2 and H_2S (left) and 100 mol% H_2 (centre, right). The valve tested at 100 mol% H_2 was cut to verify the absence of blistering or other type of damage..... 30

Figure 18. Parts of the pressure regulator after the 20 mol% H_2 exposure: membrane: general appearance (left), detail of area with unknown damaged area (centre) and cross section materialographic probe (right) showing a very superficial damage 31

Figure 19. Spirometallic gaskets after the 20 mol% H_2 + of CO_2 and H_2S impurities campaign 31

Figure 20. Parts of the pressure regulator (left) and detail of O-rings (right) after the 100 mol% H_2 campaign 31

Figure 21. Detail of membrane from the pressure regulator after the 100 mol% H_2 campaign..... 32

Figure 22. Metallic parts of the pressure regulator after the 100 mol% H_2 campaign..... 32

Figure 23. Detail of ELSTER TR22 G100 DN80 Class 600 turbine gas meter after the 100 mol% H_2 campaign 32

Figure 24. Detail of flow turbine gas meter bodies..... 33

Figure 25. Aluminum gas meter rotor and detail of rotor blade 33

Figure 26. Components of the DIDTEK 600-3 valve showing detail of the graphoil and Teflon seals after the 100 mol% H_2 campaign..... 34

Figure 27. Components of the ALFA VALVOLE n° 5 (left) and ALFA VALVOLE n° 6 (right) Teflon seals after the 100 %mol H_2 campaign..... 34

Figure 28. Components of the KURVALF rose n°2 plug valve and detail of O-ring after the 100 %mol H_2 campaign 34

Figure 29. Components of the KURVALF red n°1 plug valve showing detail of O-rings after the 100 mol% H_2 campaign..... 35

Figure 30. Photograph showing detail of the ball valve sent to TECNALIA (right) and data sheet supplied by the manufacturer (left) 36

Figure 31. Photographs showing details of the ball valve 36

Figure 32. Photographs showing detail of the deformed TFM seat..... 36

Figure 33. Photograph showing detail of the ball (left) and SEM micrograph of abraded area (centre) with EDS spectrum of this zone (right) 37

Figure 34. Test specimens inside the pig trap in the loop experimental platform at FHA at the beginning of the 2nd experimental campaign (left) and once concluded (right)..... 37

Figure 35. Test specimens inside the pig trap at the conclusion of the 100 mol% H_2 experimental campaign 38

Figure 36. Detail of tested C-ring specimens after the 100 mol% H_2 campaign 39

Figure 37. Resin embedded notched C-ring cross sections (up) and optical micrographs from steel grades X60 (down-left) and X42 (down-right) after the 2nd campaign 39

Figure 38. Optical micrograph from notched C-ring cross section of steel grade X60 after the 100 mol% H_2 campaign..... 40

Figure 39. Tested X70 base and welded 4pb specimens supported in the loading jig after the 3rd campaign (up) and tested x70 and X52 base and welded specimens after the 100 mol% H_2 campaign 41

Figure 40. Resin embedded cross sections of 4pb X52 and X70 welded steel specimens (left) and optical micrograph of metallographic section of X70 welded joint (right) after the 3rd campaign 41

Figure 41. Optical micrograph of metallographic section of X70 welded joint after the 100 mol% H_2 experimental campaign 42

Figure 42. Rack with tested CT bolt loaded specimens in experimental campaigns 2 (top-left) 3 (top-right) and 4 (down)..... 42

Figure 43. Heat tinted fracture surface of CT-WOL specimens after the 100 mol% H_2 campaign .. 43

Figure 44. Heat tinted fracture surface of X70 CT-WOL specimens after 100 mol% H₂ exposure and SEM micrograph showing detail of the fatigue pre-crack surface and crack advancing front..... 43

Figure 45. Aspect of the welded pipe sections delivered to Tecalia after the 100 mol% H₂ campaign 44

Figure 46. Magnetic particle testing of X42-X52 welded joint 45

Figure 47. Magnetic particle testing of X52-X60 welded joint 45

Figure 48. Stress strain curves of notched SSRT specimens tested in air and in H₂ (80 bar) 47

Figure 49. Electron micrographs showing fully ductile fracture surface of SSRT specimens tested in air: X52 (up-left), X60 (up-right). Numerous particles within the dimples are observed (down) 47

Figure 50. Electron micrographs of fracture surface of X52 SSRT specimen tested in H₂ at 80 bar, showing a central region with dimples generation (down-left) and a peripheral region with transgranular cleavage (down-right)..... 48

Figure 51. Electron micrographs of fracture surface of X60 SSRT specimen tested in H₂ at 80 bar (up) and detail of the peripheral region with transgranular cleavage (down) 48

Figure 52. Electron micrographs showing fracture surface of X70 SSRT specimen tested in H₂ at 80 bar (left) and detail of the peripheral region with transgranular cleavage and secondary crack penetration..... 49

List of Tables

Table 1. Description of the experimental campaign performed in the R&D facility 9

Table 2. List of valves tested in the static section of the R&D facility 14

Table 3. Details of the testing equipment in the dynamic section of the testing platform 16

Table 4. Properties of API5L steel pipes under study 17

Table 5. Types of hydrogen embrittlement test displacement specimens used in the testing platform 19

Table 6. Characteristics of SSRT tests performed at Tecalia 22

Table 7. Gas separation performance of the Membrane #2 for the tests under: (top part) same feed low and variable feed pressure; (bottom part) variable feed flow and feed pressure with the aim at maximizing the hydrogen recovery factor 29

Table 8. Summary of test results for the C-ring tests 38

Table 9. Summary of test results for the 4pb tests 40

Table 10: Summary of test results for the CT-WOL tests 44

Table 11. Summary of the results obtained in the SSR tests..... 46

Acronyms and abbreviations

ANSI	American National Standards Institute
API	American Petroleum Institute
CSA	Canadian Standards Association
CT	Compact Tension
C-ring	C-ring (specimen)
CV	Coefficient of variation
EDS	Energy Dispersive X-Ray Spectroscopy
FHA	Fundación Hidrógeno Aragón
GTAW	Gas Tungsten Arc Welding
HAZ	Heat Affected Zone
ISO	International Organization for Standardization
K_{IAPP}	Stress Intensity Factor applied to the fixed displacement WOL specimen
K_t	Stress Concentration Factor
NG	Natural Gas
NTS	Notched Tensile Strenght
OD	Outside diameter
RA	Reduction of Area
R&D	Research and development
RNTS	Notched Tensile Strenght Ratio
RRA	Reduction of Area Ratio
SEM	Scanning Electron Microscope
SSRT	Slow Strain Rate Test
TL	Transversal- Longitudinal
WOL	Wedge Opening Loading bolt loaded compact fracture mechanics specimen
YS	Yield Strenght
4pb	Four-point bend (specimen)

Executive Summary

Deliverable D4.4 gathers the results obtained in the different tests performed in all experimental campaigns, carried out in the R&D testing platform built at Fundación Hidrógeno Aragón (FHa), and the results of the slow strain rate testing (SSRT) carried out in Tecnalia's laboratory. It includes not only the last results of the experimental campaign, but also those already reported in previous deliverables (i.e. D 4.2 and D 4.3 published in the project website) to achieve a single report with the main findings of HIGGS.

The R&D facility at FHa aims to reproduce a natural gas transmission grid at smaller scale, where different testing components, materials and equipment are exposed to hydrogen. Five different types of tests/analysis have been performed, in the platform, during four experimental campaigns with hydrogen concentrations varying from 20 to 100 mol% H₂:

- Gas tightness tests of representative valves of the natural gas (NG) grid to identify possible leakages when operated with hydrogen.
- Constant displacement tests carried out on API 5L steel specimens grades X42, X52, X60 and X70, for hydrogen embrittlement evaluation of representative carbon steels in the NG grid. Three types of constant displacement specimens have been produced: C-ring, four-point bend (4pb) and compact tension (CT) wedge opening loading (WOL) specimens.
- Inspection of the valves and components from the pressure regulator and filter for hydrogen damage evaluation. These components were evaluated after each experimental campaign. At the conclusion of the 100 mol% H₂ campaign, the turbine gas meter was also inspected.
- Inspection of welded sections of the API 5L steel pipes under study, at the conclusion of the four experimental campaigns. The magnetic particle testing method has been used, in the welded joints, to detect surface-breaking discontinuities, such as cracks and pits.
- H₂/CH₄ gas separation tests with a Pd-based membrane prototype, performed during the 1st experimental campaign (i.e. 20 mol% H₂ in CH₄).

In combination with the constant displacement (constant load) tests, rising load tests have been carried out in Tecnalia's laboratory. The SSRT tensile method has been used as a valuable primary screening method of materials.

Table 1 summarises the composition of the gas atmosphere used in each of the experimental campaigns, as well as the type of tests carried out.

Table 1. Description of the experimental campaign performed in the R&D facility

CAMPAIGN N°	GAS COMPOSITION	TYPE OF TEST	PRESSURE (bar)	TEST DURATION (h)
1	20 mol% H ₂ 80 mol % CH ₄	<ul style="list-style-type: none"> Gas tightness Gas separation Hydrogen embrittlement: constant displacement tests Inspection of equipment & valves 	80	2200-3000
2	20 mol% H ₂ 4 mol% CO ₂ 11 ppmv H ₂ S 76 mol % CH ₄	<ul style="list-style-type: none"> Gas tightness Hydrogen embrittlement: constant displacement tests Inspection of equipment & valves 		
3	30 mol% H ₂ 4 mol% CO ₂ 11 ppmv H ₂ S 66 mol % CH ₄	<ul style="list-style-type: none"> Gas tightness Hydrogen embrittlement: constant displacement tests Inspection of equipment & valves 		
4	100 mol% H ₂	<ul style="list-style-type: none"> Gas tightness Hydrogen embrittlement: constant displacement tests and SSRT tests Inspection of equipment, valves and welded sections of API 5L pipes 		

The most significant results obtained in the different tests carried out at HIGGS are summarised below:

- Most of the testing values remained tight for the duration of the test, with just minor hydrogen losses due to hydrogen preferential permeation, through the body of screwed ball and needle valves. The analysis of the ball valve with a leakage, at the end of the 2nd campaign, was due to a clear misalignment between the ball of the valve and the Teflon seat, and not to hydrogen permeation.
- The results of the inspection carried out in the valves, pressure regulator, cartridge filter and turbine gas meter components showed no damage due to their exposure to the different hydrogen mixtures. Only in the 30 mol% H₂ campaign, a significant blistering was observed in a valve seat, not detected however, in the 100 mol% H₂ level. There is therefore, no clear evidence of the influence of hydrogen on the observed damage.
- The membrane prototype has shown a great gas separation performance. It has been validated for 1Nm³/h feed mix gas mixture (20 mol%H₂-80mol%CH₄ gas blend), being stable for around 500h of continuous operation, with a maximum H₂ purity of 99.5 mol%.
- The magnetic particle inspection method carried out in the welded pipe sections of the API5L steels under study, did not show discontinuities, such as cracks in the internal surface of the welded joints that were exposed, during approximately 11000 hours, to the different hydrogen concentrations.
- With respect to the hydrogen embrittlement tests, the C-ring and 4pb constant displacement specimens machined from the API5L steel pipes under study, did not show cracking when exposed to the different hydrogen gas compositions, at 80 bar pressure, and test duration up to 3000 hours. No crack propagation was also noticed in CT-WOL specimens. The results of the SSRT tests yielded values of the notched tensile strength ratio categorized as low

D4.4 Final report on systematic validation of testing loop

sensitivity to hydrogen embrittlement. The results obtained are therefore, indicative of low susceptibility to hydrogen embrittlement for API 5L steels grades X42, X52, X60 and X70, in the tests conditions established in HIGGS.

The tested elements have shown therefore, compatibility with hydrogen levels up to 100 mol% H_2 , under the specific conditions considered in HIGGS.

1 Objectives

The main objective of this deliverable is to gather and analyse all the results obtained, in the four experimental campaigns, carried out at the testing platform at FHa, as well as in the SSRT, performed in Tecnalia's laboratory.

More specifically, the objectives of this document are:

- To check the gas tightness of representative valves from the European transport NG grid.
- To evaluate the compatibility with hydrogen of significant components and equipment of pressure regulation and/or metering stations.
- To evaluate a potential hydrogen embrittlement damage in API 5L base and welded steel pipes grades X42, X52, X60 and X70.
- To check the gas separation performance of a Pd-based membrane prototype.

2 Introduction

Blending hydrogen with NG may have an impact on safety issues, pipeline integrity, and gas quality. The potential leakage rate of hydrogen is much larger than that of NG through the same sized leak. Besides, possible hydrogen embrittlement mechanism may occur under the transport pressures and the combustion properties change when hydrogen is added to NG, with direct impact on end users.

Research to assess the impact of hydrogen on the NG infrastructure is therefore necessary when analysing its suitability for hydrogen transport, with special focus on hydrogen embrittlement and gas leakage. Gas separation technologies are also necessary to obtain high-concentrated methane streams, from admixture flows below 20 mol% H₂.

Hydrogen embrittlement is a process, in which the tensile ductility of a material working on hydrogen environment is significantly reduced, because of the introduction of hydrogen atoms in its lattice. Additionally, the fracture toughness and fatigue strength of this material decreases. The severity of these manifestations of hydrogen embrittlement depends on mechanical, environmental and material (microstructure and tensile strength, principally) variables. It is critical to ensure the resistance of pipelines materials and other metallic materials in the grid to this phenomenon, for a safe and efficient hydrogen transport.

The testing platform built at FHa is an R&D setup that tries to replicate a NG transmission facility in which real pipes, components and equipment of high-pressure grids have been installed to expose them to hydrogen blends at 80 bar pressure, to assess the suitability of high-pressure NG grids for the transport of H₂/NG blends or even 100 mol% H₂ gas. For this purpose, gas tightness tests, constant displacement mechanical tests and gas permeation tests are carried out in the HIGGS project. Also, and because end users could not be able to accommodate high levels of hydrogen if gas is transported as a blend, a Pd-based membrane prototype was developed in HIGGS to deal with H₂/CH₄ separation.

As a complement to the hydrogen embrittlement tests carried out in the R&D platform under constant load/constant displacement, dynamic / increasing displacement tests have been carried out in Tecnalia's laboratory. The SSR tensile test method has been used as a valuable primary screening method of materials.

3 Test methods for the testing platform at FHa

The R&D testing platform designed and built in the frame of the HIGGS project, consists of a static section, a dynamic section, and a membrane prototype. A picture of this facility can be seen in Figure 1. The static section is the part of the facility where the tightness of valves is studied. In the dynamic section, the impact of hydrogen on the material integrity of pipes and equipment is assessed. Finally, gas separation tests are performed with a membrane prototype to recover hydrogen from the high-pressure blend.



Figure 1. Picture of HIGGS experimental platform at Aragon Hydrogen Foundation (FHa, Spain)

3.1 Gas tightness tests

The tightness of several valves towards hydrogen has been tested in the static section of the testing platform. Plug, needle, ball, and butterfly valves were selected in WP3 as the most representative valves in the grid, and they were installed in the platform with flanged and screwed couplings. In each line of the static section up to three testing valves were installed. Each line was equipped with a pressure transmitter and an analysis port to monitor the pressure level and the hydrogen concentration, in the line during the test, respectively. A detail of the valves testing section is given in Figure 2.

The lines were fed with gas at 80 bar and isolated afterwards. The lines stayed in a static way full of gas for each experimental campaign. During the test, the pressure was monitored, and the admixture composition checked periodically using a gas analyser.

Specific information about the testing valves is given in Table 2.



Figure 2. Picture of the valves testing section

Table 2. List of valves tested in the static section of the R&D facility

Element	Manufacturer	Model	Coupling
Ball Valve	ALFA VALVOLE	ALFA-606/FB Split Body	Flanged
Lug-type butterfly Valve	DIDTEK	Lug-zero leakage class	Flanged
Plug valve	KURVALF	RF-VP	Flanged
Needle valve	ALFA VALVOLE	A20T 800LB	Screwed
Ball valve	NUOVAFIMA	BSV/VV	Screwed

At the end of the gas tightness tests, the flanged valves were disassembled, and their different parts inspected to detect the presence of cracks or any other damage, that could be attributed to hydrogen exposure.

3.2 Gas separation test

Membrane technology was used in HIGGS to deal with H₂/CH₄ separation. Pd-based double-skinned membranes deposited onto 14 mm outside diameter (OD) porous ceramic tubes were prepared and integrated in the membrane prototype for this study, following the preparation procedure reported in [1]. Two tests have been performed in HIGGS.

The first one was carried out by using Membrane #1 with 22.1 cm long and the second one by using Membrane #2 of 21.7 cm long. Pd-based membranes have been selected because of their high hydrogen permeance and selectivity compared to other materials. The gas separation prototype consists in three parts: 1) the feed section, where the blend prepared in the admixture system of the

D4.4 Final report on systematic validation of testing loop

R&D platform is delivered at high pressure to the membrane module, 2) the membrane reactor, where the membranes are allocated and the operating temperature of 400 °C is achieved with an oven and 3) an analysis section to check the composition and quantity of the separated flows.

The prototype consisted in a feeding line as inlet and two outlets (permeate and retentate). The permeate was the stream rich in hydrogen, and the retentate, rich in methane, Figure 3. A back-pressure regulator was placed at the outlet of the retentate side to set the required trans-membrane pressure difference. The retentate and the permeate lines were connected to the analysis section with mass flow meters, to measure and monitor the permeate and retentate flows.

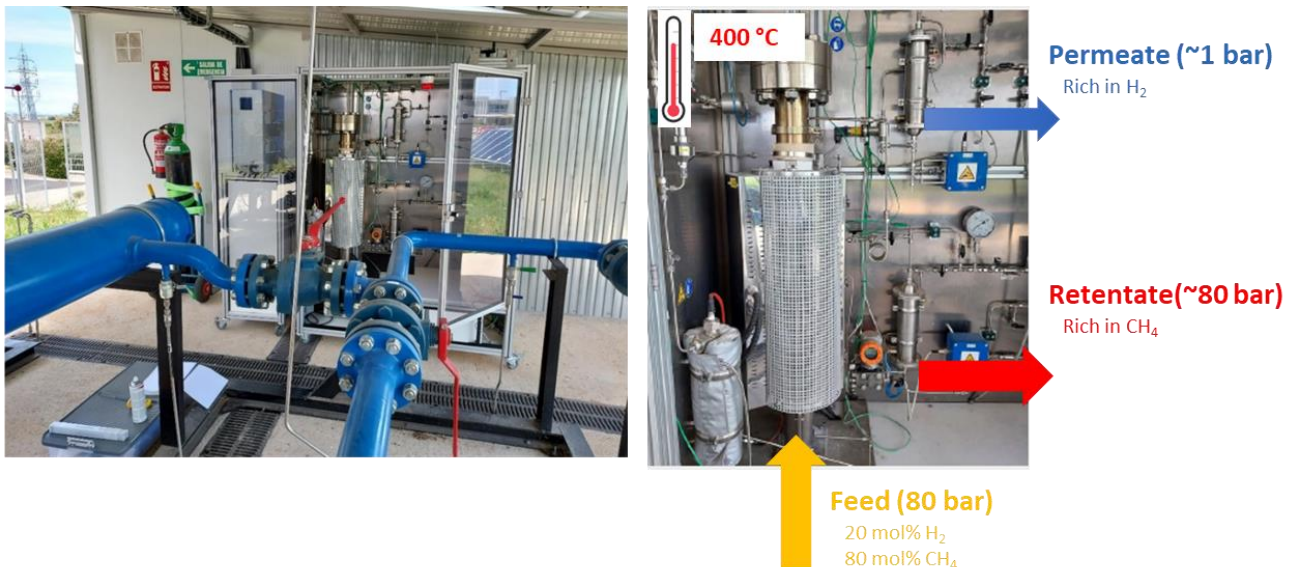


Figure 3. Gas separation prototype

In a first experiment, the long-term stability of this kind of membranes was tested under a constant feed flow ($8.3 \text{ NI}\cdot\text{min}^{-1}$) and feed pressure (80 bar). In a second round of tests, the feed pressure was varied (10, 20, 40, 60, 80 bar) and then, feed flow was tuned for obtaining the maximum H_2 recovery for each feed pressure.

With the first membrane, mixed gas tests were performed at 400 °C, feeding $8.33 \text{ NI}\cdot\text{min}^{-1}$ of the H_2/CH_4 blend (20%mol H_2) at 80 bar to the membrane module. The mixed gas test consisted in 5 cycles of 100 hours each, maintaining the system at operating pressure but without feed flow between cycles. The permeate flow and hydrogen content, in the permeate stream, were monitored to assess the gas separation performance of the membranes.

With the second membrane, feed flow and pressure were modified between $1.12\text{-}6.15 \text{ NI}\cdot\text{min}^{-1}$ and 10-80 bar for the mixed gas tests, respectively, maintaining the operating temperature always at 400 °C. The permeate flow and hydrogen concentration, in the permeate stream, were monitored to calculate the hydrogen recovery. The whole experiment lasted 175h.

The gas separation tests have been only carried out in the first experimental campaign, since this campaign does not incorporate impurities that could damage the membrane.

3.3 Inspection of valves and equipment after H₂ exposure

At the end of each experimental campaign, the following components were inspected:

- The flanged valves: after the gas tightness tests the valves were disassembled, and their different parts inspected to detect the presence of cracks or any other damage, that could be attributed to hydrogen exposure.
- Components and equipment located in the dynamic section of the testing platform (Figure 4): the cartridge filter, the pilot-pressure regulator, and the turbine gas-meter, were disassembled and their different parts (membranes, O-rings, filters...) inspected. The turbine gas meter was only characterised at the end of the 100 mol% H₂ exposure.
- The ball valve which showed a leakage at the end of the 2nd experimental campaign (see Table 1).

The characteristics of the valves under study have already been shown in Table 2. The properties of the equipment from the dynamic section are shown in Table 3.

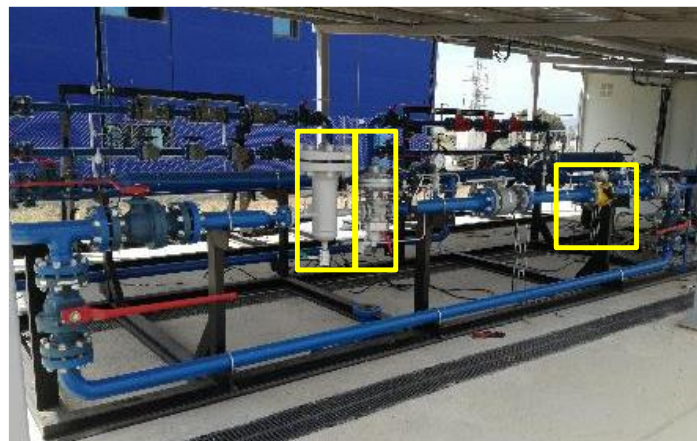


Figure 4. Picture of the testing equipment in the dynamic section

Table 3. Details of the testing equipment in the dynamic section of the testing platform

Element	Manufacturer	Model
Cartridge filter	FIORENTINI	HFA/1 REFLUX-819
Pilot-operated pressure regulator	FIORENTINI	P.207/A+R14 SB-105
Turbine gas-meter	ELSTER	TR22 G100 A1R/A 1S
Pressure indicator	NUOVAFIMA	MGS18/2/A EJA530E-JCS7N-014EN
Pressure transmitter	YOKOGAWA	KU22
Temperature transmitter	YOKOGAWA	YTA610

3.4 Hydrogen embrittlement tests

Hydrogen embrittlement tests were carried out on API 5L [2] qualities grades X42, X52, X60 and X70. A picture of the API 5L X70 steel pipes under study is given in Figure 5. The chemical composition, mechanical properties and metal microstructure of the as received base and welded steels were characterised. It is important to note that the API 5L steels under study are new materials, this is, they have not been in service. Table 4 summarises important aspects of the steels under study. The heat affected zone (HAZ) and weld metal regions corresponding to a X70 steel welded joint are shown in Figure 6, together with the hardness evolution in the above-mentioned regions.



Figure 5. Detail of sections of the API 5L X70 steel pipes upon reception in Tecalia

Table 4. Properties of API5L steel pipes under study

API 5L steel grade	Outside diameter (mm)	Wall thickness (mm) ¹	Yield strength (MPa)		Ultimate tensile strength (MPa)		Welding procedure /filler material	Microstructure (base steel)
			Tensile testing (ISO 6892) [1]	API 5L (min.)	Tensile testing (ISO 6892)	API 5L (min.)		
X42	168	6.9	451	290	542	415	GTAW ² /ER70S-6	Ferrite + pearlite
X52	168	7.8	440	360	514	460	GTAW/ER70S-6	Ferrite + pearlite
X60	168	7.8	510	415	581	520	GTAW/ER90S-B3	Bainite
X70	406	8.2	549	485	675	570	GTAW/ER90S-B3	Ferrite + bainite

¹Measured in metallographic probe; ²GTAW: Gas Tungsten Arc Welding

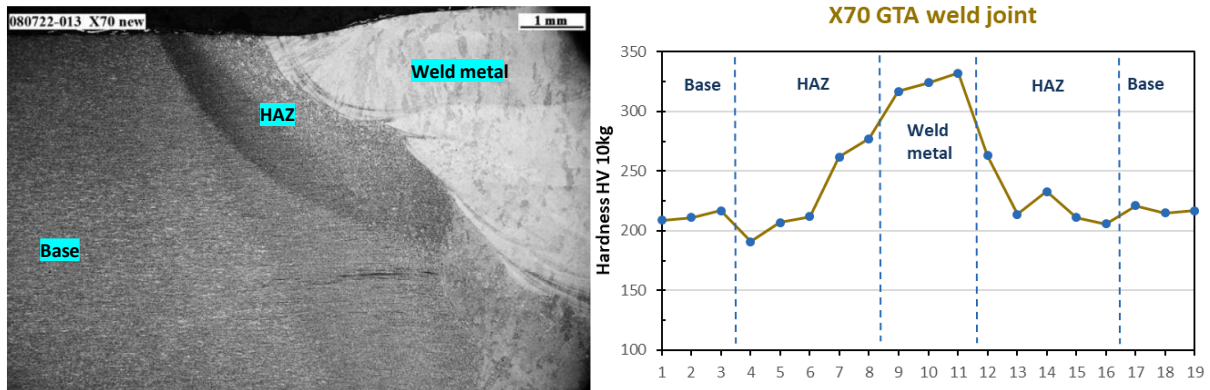


Figure 6. Optical micrograph showing detail of cross section of GTA welded joint in X70 steel (left) and micro-hardness evolution in this welded joint (right)

3.4.1 Constant displacement tests at FHA

The tests on steels have been performed using constant displacement specimens mechanised from the base and welded API 5L steel pipes. The displacement initially applied to the specimen is held constant throughout the duration of the test. An important benefit of using constant strain specimens is that, once the deformation has been applied to the specimen, the self-loading assemblies may be inserted into loops or closed test vessels and exposed to the hydrogen environment, at a certain pressure, Figure 7. The development of a pig trap in the dynamic section of the testing platform, aiming as an autoclave that can operate at 80 bar, gives an opportunity to evaluate constant loaded specimens, for times significantly longer (up to 3000 hours) than those typically used in rising load tests, such as SSRT, fracture toughness or fatigue tests.

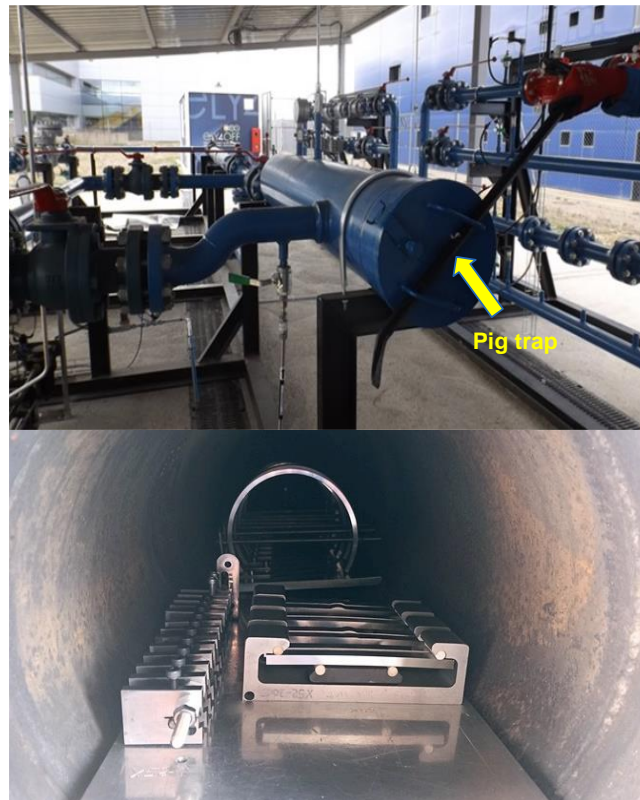


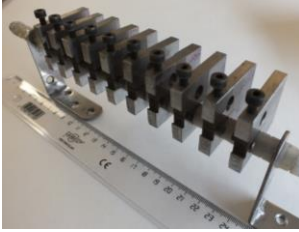


Figure 7. Picture of the pig trap (up) and the constant strain specimens allocated inside it (down)

D4.4 Final report on systematic validation of testing loop

Three types of normalised constant displacement specimens have been produced in HIGGS: C-ring, 4pb and CT-WOL specimens. Details of the three normalised constant displacement specimens are summarised in 5.

Table 5. Types of hydrogen embrittlement test displacement specimens used in the testing platform

Type of specimen	Constant displacement specimens		
	C-ring	4pb	CT-WOL
Geometry			
Condition	Smooth and notched base specimens	Base and welded specimens	Fatigue pre-cracked base and welded
Applicable standards	ISO 7539-5, ASTM G38	ISO 7539-2, ASTM G39	ISO 7539-6, ASTM E1681
Atmosphere	20-30 mol % H ₂ + CH ₄ / 100 mol % H ₂		
Pressure	80 bar		
Test duration	2300-3000 hours		
Post testing evaluation	<ul style="list-style-type: none"> ➤ Evidence of cracking in C-ring and 4-pb specimens ➤ Crack growth in CT-WOL specimens 		
Advantages	<ul style="list-style-type: none"> ➤ Once loaded the specimens are inserted in the pig trap and exposed to the H₂ environment for long periods of time 		

C-rings specimens were strained to the 100% of the yield strength (YS). Due to the circumferential welding of the pipe sections, C-ring specimens have only been machined out from base X42, X52 and X60 (OD 168mm). It has been not possible to produce C-rings specimens from the X70 406mm OD pipe. The designing, machining and loading process for C-ring specimens has been carried out according to ISO 7539-5 [3] and ASTM G38 [4] standards.

4pb base and welded specimens are flat strips of metal of uniform rectangular cross section and uniform thickness, except in the welded specimens where testing is specified with one face in the as-welded condition. The 4pb specimen is subjected to a constant displacement that is performed by supporting the beam specimen on two loading rollers and applying a load through two other rollers, so that one face of the specimen is in tension and the other is in compression. Similar to the C-ring specimens, 4pb specimens were strained to the 100% of the elastic limit. Indications for the preparation and use of 4pb specimens are given in ISO 7539-2 [5] and ASTM G39 [6] standards.

The CT-WOL fatigue pre-cracked (in air) specimen described in ASTM E1681 [7] and ISO 7539-6 [8] is well suited for constant displacement tests. It can be self-loaded by tightening a bolt against a taper pin, to produce a constant displacement at the loading points. The maximum stress intensity factor (K_{IAPP}) applied to the CT-WOL specimen can be estimated according to ASTM E1681. The force (P) to be applied is calculated from the selected K_{IAPP} . The machined notch is oriented in the

D4.4 Final report on systematic validation of testing loop

TL (transversal-longitudinal) direction. In the case of the specimens used in HIGGS, there is an important size limitation due to the small wall thickness of the as received API 5L steel pipes. To be able to use higher K_{IAPP} values, the CT-WOL geometry used in the 3rd and 4th campaigns was slightly modified in comparison to that defined in the 1st and 2nd campaigns. Besides, the CT-WOL specimen is considered by ASME B31.12 [9] as a testing method for materials qualification in hydrogen.

The C-ring, 4pb and CT-WOL specimens are kept in the loaded condition in the hydrogen gas blend during all the duration of the test. At the conclusion of each experimental campaign, the specimens were unloaded. The evaluation of the steel resistance to hydrogen embrittlement was realized by visual examination, at the conclusion of the tests, for crack detection, followed by metallographic examination of cross sections. The CT-WOL specimens, once unloaded, were heat tinted (300 °C/30 minutes), then broken, and the fracture surface was examined by Scanning Electron Microscope (SEM) to assess if subcritical cracking occurred from the initial fatigue pre-crack. According to ASTM E1681 standard, there is no fatigue pre-crack growth if the average measured crack growth does not exceed 0.25 mm.

3.4.2 Hydrogen exposure of welded API 5L

Some sections of the API 5L steel pipes grades X42 to X70 under study were welded to each other following the GTAW procedure and installed in the R&D facility at FHA (Figure 8). The objective was to check the effect of hydrogen on both, the welded and the parent material, after the approximately 11000 hours of exposition to the different hydrogen concentrations used in the four experimental campaigns carried out.



Figure 8. Welded pipe sections of the API 5L steel pipes

At the conclusion of the 100 mol % H₂ campaign, the welded sections were cut and sent to Tecnia for inspection, to detect the presence of cracks. The inspection was carried out by the non-destructive magnetic particle testing, following the ISO 17638 [10] standard. This method allows detecting surface-breaking discontinuities in ferromagnetic materials, such as cracks and pits. It consists of magnetising the part to be inspected, applying magnetic particles (fine powder of iron filings) and evaluating the accumulation of these particles around the discontinuities, making them visible to the naked eye when using a fluorescent medium.

3.4.3 Slow Strain Rate Tests


As a complement to the constant displacement test specimens used for the evaluation of hydrogen embrittlement sensibility, a rising load test method, such as the SSRT, was proposed for the API 5L steels under study. The SSRT is a particularly important screening method to measure susceptibility to hydrogen embrittlement. Specimens are tensile strained to failure with “slow” strain rates, commonly in the range 10^{-6} - 10^{-4} s⁻¹. The results of the SSRT are evaluated comparing the results obtained in an inert environment (air/N₂/He) and in hydrogen gas. The reduction of area (RA) ratio and the notched tensile strength (NTS) ratio are used as a measure of hydrogen susceptibility in smooth or notched specimens, respectively. In the case of the API 5L steels under study, notched tensile specimens were used to amplify the effect of hydrogen assisted fracture. Tests were carried out in H₂ gas (99.999%), at 80 bar, and using a strain rate of 10^{-6} s⁻¹, following ASTM G142 [11] and ASTM G129 [12] standards.

Figure 9 shows a detail of the SSRT, fracture toughness and fatigue machine for testing in H₂ gas. A picture of the notched tensile specimens used in HIGGS is shown in Table 6. The stress concentration factor (K_t) due to the notch in the (base) notched specimens is 4.6. K_t is defined as the ratio between the peak stress at the root of the notch, and the nominal stress which would be present if a stress concentration did not occur.



Figure 9. SSRT, fracture toughness and fatigue machine for testing in H₂ gas (left). Detail of fractured notched specimen (right)

Table 6. Characteristics of SSRT tests performed at Tecnia

Type of specimen	Rising load test
	SSRT
Geometry	
	Notched tensile specimens
Applicable standards	ASTM G142/G129, ISO 7539-7 [11]
Atmosphere	100 mol% H ₂
Pressure	80 bar
Test duration	7-14 hours
Post testing evaluation	<ul style="list-style-type: none"> ➤ Reduction of Area (RA); Ratio RA (RRA) ➤ Notched Tensile Strength (NTS); Ratio NTS (RNTS)
Advantages	<ul style="list-style-type: none"> ➤ Material screening method ➤ HEE indexes could be established based on the RA and NTS ratios

4 Results from the experimental campaign

The following subsections contain the results of the different tests performed according to the methodology described in section 3.

4.1 Gas tightness tests

The evolution of the pressure and the composition of the gas, for each line of the static section, during the time of the experiment, for the four experimental campaigns, is given in Figure 10 to Figure 13. Two possible losses are possible: 1) decrease in pressure level would stand for a critical tightness failure and 2) decrease in the hydrogen concentration in the blend would mean that hydrogen is being lost, due to its preferential permeance over methane. There are three lines that allow to discriminate the losses by general parts of the installation. The reference line contains no testing element at all is the blank test. Two other lines include just flanged or screwed couplings. These lines help to distinguish whether a possible leakage comes from the coupling or the body of the valve. The methodology followed is detailed in section 3.1.

The main results obtained in the four experimental campaigns are summarised below.

4.1.1 Testing Campaign #1: 20 mol% H₂ /80 mol% CH₄

Figure 10 shows no critical pressure losses in any branch of the static section. The pressure oscillates slightly (76.7±4.5 bar is the biggest interval for the line with flanged ball valves) due to temperature changes from day to day, as well as between night and day. The hydrogen content remains basically constant in the three reference lines, being the oscillation shown within the measuring error of the analyser (<1%mol) and in all cases below 0.5%mol. Neither the line itself nor the couplings (flanged or screwed) show relevant hydrogen losses and the whole system can be considered tight. Thus, all the valves tested in this campaign, can be considered ready for operation under the 20mol%H₂ /80mol% CH₄ hydrogen blend.

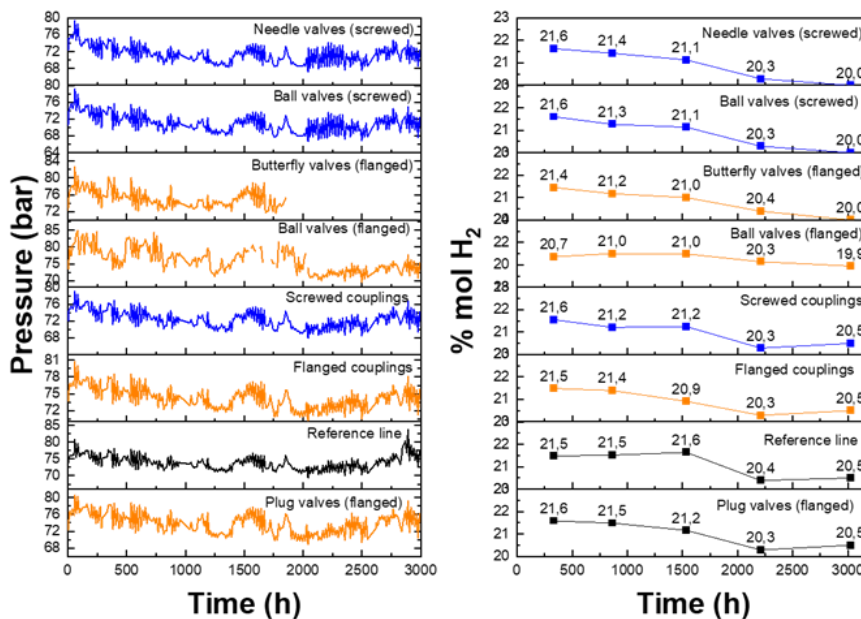


Figure 10. Evolution of the pressure (left), and H₂ gas composition (right) in each line of the static section during the 1st experimental campaign (20 mol% H₂)

4.1.2 Testing Campaign #2: 20 mol% H₂/4 mol% CO₂/11 ppmv H₂S/76 mol% CH₄

During the 2nd experimental campaign, a new temperature transmitter was incorporated to correct pressure oscillations due to temperature changes. The evolution of the pressure and the hydrogen concentration (%mol H₂) for each line of the static section is given in Figure 11. Pressure variation is plotted as P/Z·T versus time to check the evolution of this ratio during the test. This quotient must remain constant in a close system as long as no gas flows out of the system. The compressibility factor has been calculated using the API Soave-Redlich Kwong equation of state, for each pressure and temperature value registered, by the transmitters in the platform (see section 5.1 in Deliverable 4.2 for more details).

Although most valves and couplings remain tight, a critical leakage was detected in all the lines containing flanged valves. These valves were disassembled after the 1st experimental campaign and reassembled again, probably not precisely enough to ensure the tightness of the valves. It is therefore concluded that the reassembly of the valves should be done by the manufacturer expertise. Regarding the hydrogen concentration in the lines, it remains approximately constant during the entire test, with slightly fluctuating values around 24.5%mol, coherent with the measuring error range of the gas analyser. In fact, in certain valves the hydrogen level seems to increase as the test advances. This fact may be indicative of hydrogen stratification in the line since the points where the samples are taken, are located at the top of the pipes, although evidence is not sufficient for such statement.

At the conclusion of the test a critical gas leakage was detected in one screwed ball valve, after emptying the platform. The analysis of this ball valve is detailed in section 5.4.1 of this deliverable. It was concluded that, the most likely cause of the leakage observed in the ball valve, was due to a misalignment between the ball and one of the Teflon seats, and cannot be attributed to a hydrogen damage.

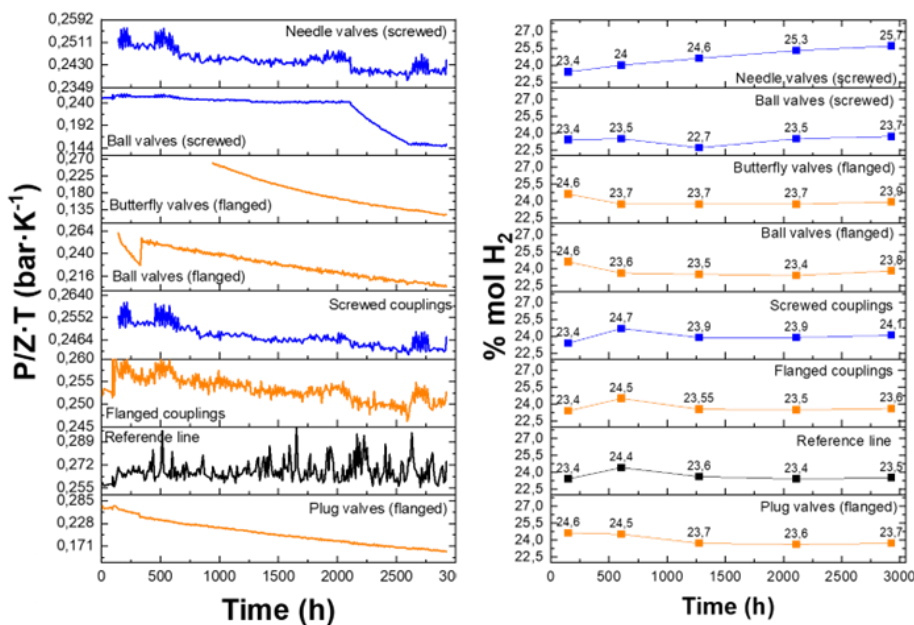


Figure 11. Evolution of the pressure P/Z·T quotient (left) and H₂ gas composition in each line of the static section during the 2nd experimental campaign (20 mol% H₂ + impurities of H₂S and CO₂)

4.1.3 Testing Campaign #3: 30 mol% H₂/4 mol% CO₂/11 ppmv H₂S/66 mol% CH₄

The evolution of the pressure and the hydrogen concentration for each line of the static section, during the 3rd experimental campaign, is given in Figure 12. It can be seen how most valves and couplings remained tight, since the P/Z·T values were constant enough during the test, with values around 0.25-0.27 bar·K⁻¹ and standard deviation and CVs below <0.005 bar·K⁻¹ and 0.008, respectively.

A clear pressure drop was detected in the line containing the screwed ball valves. This leak was, however, caused by a sudden change in the setpoint of a pressure relieve valve (a safety item in the line) and not to the malfunction of these testing valves. A small leak, undetected by the gas detector, occurred also in the flanged ball valves. This leak was not worrying since it led to a standard deviation of 0.004 bar·K⁻¹ and a CV of 0.005 in the P/Z·T value.

Similar to what was observed in the 2nd experimental campaigns, a slight increase in H₂ concentration was detected as the test advances. However, the increase is not high enough to assume that hydrogen stratification in the line, was occurring.

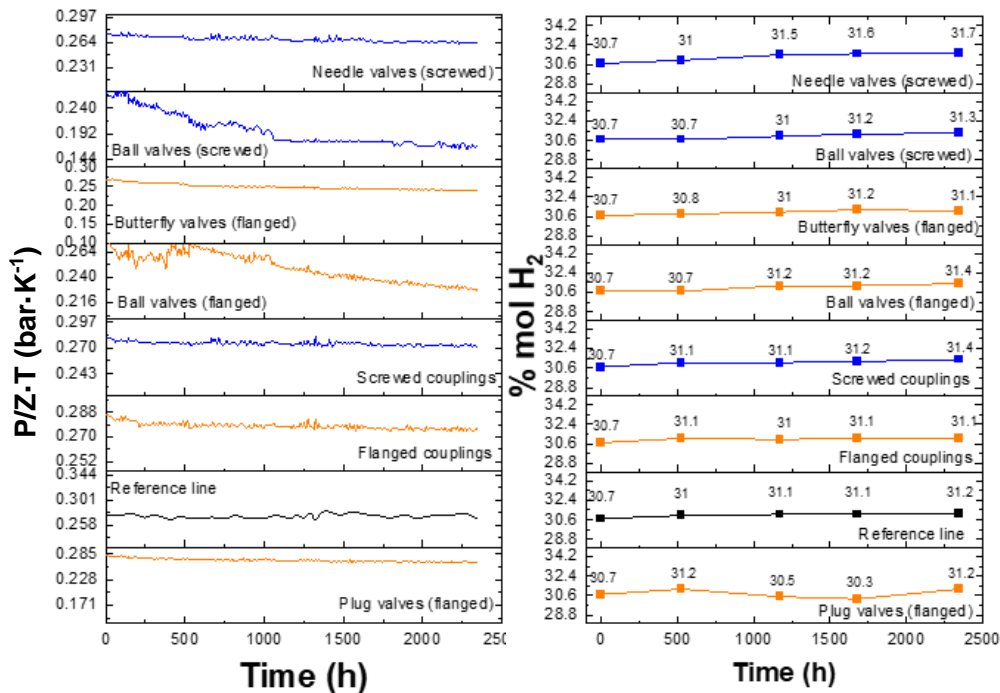


Figure 12. Evolution of the pressure P/Z·T quotient (left) and H₂ gas composition in each line of the static section during the 3rd experimental campaign (30 mol% H₂+ impurities of H₂S and CO₂)

4.1.4 Testing Campaign #4: 100 mol% H₂

The evolution of the pressure in each line of the static section during the 100 mol% H₂ campaign, is given in Figure 13. In this case, only the evolution of the P/Z·T ratio is depicted since no blend has been injected in the setup, for this test.

All lines were tight to hydrogen during the test, with standard deviations <0.01 bar·K⁻¹ and CVs <0.008 in all P/Z·T values. Noteworthy, these statistical values are basically double that for the campaign considering the 30 mol% H₂ blend (3rd experimental campaign). The result is logical because

D4.4 Final report on systematic validation of testing loop

of the high content of hydrogen in the line, with its high diffusivity, but means no critical pressure loss yet.

A clear drop in the flanged plug valves (undetectable by the gas detector) was observed during the test. After 1000h, the line was feed again with hydrogen to ensure the result and the tendency repeated. The problem was identified in one of the three testing valves, which was not tight to hydrogen, although the accurate point of leakage could not be found. The other two functioned correctly. A small pressure drop was also observed in the flanged butterfly and ball valves, also undetectable by the gas detector, meaning no big deal for the overall tightness of the system.

Finally, once the test ended, the gas composition in the lines was analysed before emptying them, and no traces of methane from previous tests were detected. Therefore, either methane has not been adsorbed by the pipes in the previous campaigns, or it was not released during operation with 100 mol% H₂. In any event, hydrogen was not polluted during the last test.

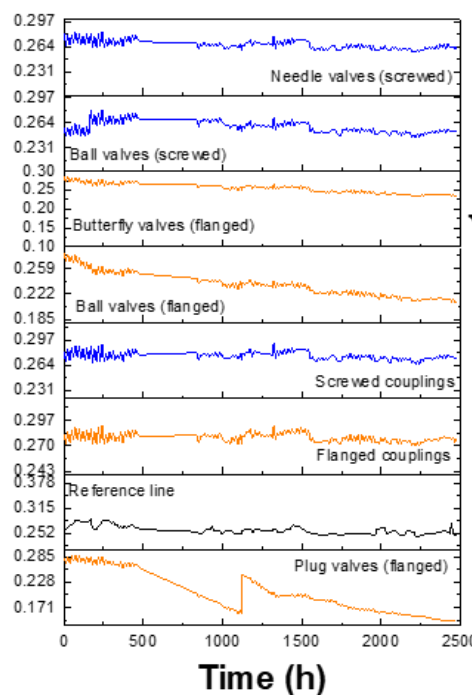


Figure 13. Evolution of the pressure $P/Z \cdot T$ in each line of the static section during the 4th experimental campaign (100 mol% H₂)

An additional test was performed with the flanged valves to check their internal tightness, when operating with 100 mol% hydrogen. Just one plug, ball and butterfly valve were selected for this test. At the beginning of the test, hydrogen was fed at 70 bar to one side of the valve and the other side was left at atmospheric pressure. The pressure evolution was monitored at the low-pressure side during several hours.

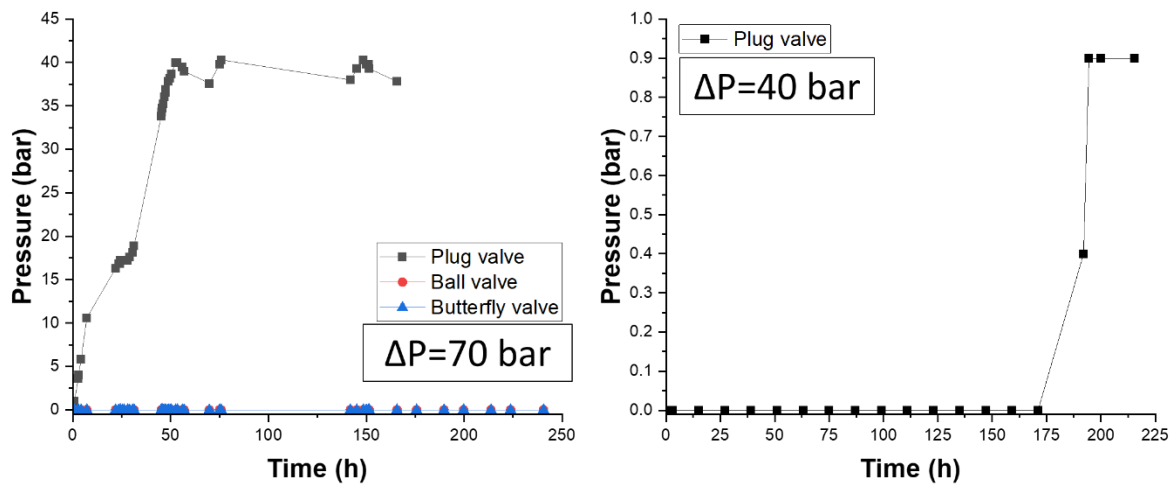


Figure 14. Pressure against time during the internal tightness test at $\Delta P=70$ bar (left) and $\Delta P=40$ bar (right)

Figure 14 shows the results of the internal tightness test. It can be seen how hydrogen did not leak internally for the ball and butterfly valves, since the pressure level at the low-pressure side of the valve remained as 0 bar during the 250 h of the test. There was, however, a clear leakage for the plug valve, where the pressure, at the low-pressure side, rises continuously until reaching 40 bar in around 60 h. A second test was performed with a different plug valve, feeding the high-pressure side at 40 bar. In this case, the valve remained completely tight for 173 h, when a small pressure increase was detected (see Figure 14-right).

The malfunction of the plug valve seems related to the lack of tightness already detected in the external tightness tests. Since this malfunction has only happened with one valve, there is not sufficient evidence to state that this kind of plug valves are not suitable for service under 100 mol% H₂. It would be advisable however to perform complementary tests with valves of the same nature to reach a clearer conclusion.

4.2 Gas separation performance of the membrane prototype

The separation of the 20 mol% H₂/ 80 mol% CH₄ blend was performed with a gas separation prototype that used Pd-based membranes (see details in section 3.2). The gas separation performance of the prototype with Membrane#1 for the 500h operation is shown in Figure 15.

The permeate flow (rich in hydrogen) has been monitored and its composition analysed periodically during the different cycles of the test. Figure 15 shows how the permeate flow remains mainly constant during the whole operation, with an average value of 1.35 ± 0.06 NI·min⁻¹. The hydrogen content in the permeate stream is of 98.6 %mol at the beginning of the test but, decreases gradually from the second cycle on. Its values are anyway always above 96.0 %mol. The retentate stream can be calculated with a mass balance because the composition of the feed and permeate flows is known. A retentate flow of 6.93 to 7.03 NI/min⁻¹ with a hydrogen content between 3.5 and 5.7 %mol can be calculated. The CH₄ content in the retentate flow (between 94.3-96.5%mol) may be sufficient for end-users demanding a high natural gas quality. In any event, the CH₄ content in the retentate stream could be raised by increasing the membrane area if deemed necessary.

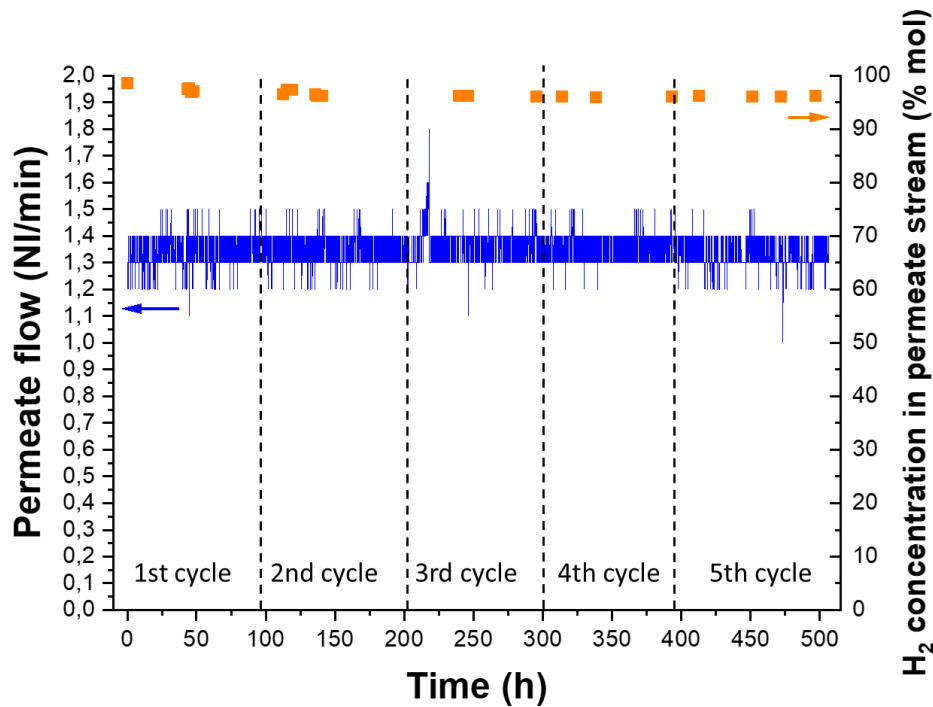


Figure 15. Gas separation performance of the prototype with Membrane #1. Blue line stands for the total permeate flow and orange scatter stands for the H₂ purity in the permeate stream

Gas separation tests were also performed with Membrane #2. Firstly, the feed flow was maintained at 8.3 NI/min and feed pressure was varied (Table 7– top). Then, the feed flow was modified for each feed pressure during the test to tune the permeate stream towards obtaining the maximum hydrogen recovery possible (Table 7–bottom). The permeate flow (rich in hydrogen) was monitored and its composition analysed periodically during the different cycles of the test. The obtained results about H₂ content in the retentate and permeate streams and hydrogen recovery are summarised in Table 7. The decrease of the feed flow maintaining the feed pressure increases the hydrogen flow in the permeate, subsequently increasing the hydrogen recovery rate and reducing the hydrogen content in the retentate stream. The hydrogen purity in the permeate stream was higher than 99.5 mol% after the 175 hours of the testing campaign and, therefore, a hydrogen concentration value down to 2.7 mol% was achieved in the retentate stream, when tuning the operating conditions. This was the highest hydrogen recovery value obtained.

Table 7. Gas separation performance of the Membrane #2 for the tests under: (top part) same feedflow and variable feed pressure; (bottom part) variable feed flow and feed pressure with the aim at maximizing the hydrogen recovery factor

Total feed flow (NI/min)	Feed pressure (bar)	H ₂ content permeate (mol %)	H ₂ content retentate (mol %)	H ₂ recovery (mol %)
8.30	10	99.9	14.9	30.1
8.30	20	99.8	10.3	54.1
8.30	40	99.6	7.8	66.0
8.30	60	99.5	6.6	71.9
8.30	80	99.5	5.3	77.9
Total feed flow (NI/min)	Feed pressure (bar)	H ₂ content permeate (mol %)	H ₂ content retentate (mol %)	H ₂ recovery (mol %)
1.12	10	99.8	12.2	44.6
2.24	20	99.8	7.6	66.9
3.12	40	99.6	4.8	79.9
4.63	60	99.5	3.4	85.9
6.15	80	99.5	2.7	90.0

4.3 Results of equipment from the dynamic section

The pilot-operated pressure regulator and the cartridge filter tested in the dynamic section of the testing platform, were disassembled at the end of each experimental campaign and their different parts examined. At the conclusion of the 100 mol% H₂ experimental campaign (i.e. 4th campaign), the turbine gas meter was also inspected. See section 3.3 for more details.

A visual inspection of the items under study was carried out by Tecnalía with the aid of a stereo microscope with a camera, to detect cracking or other type of hydrogen damage, such as blistering. It cannot be excluded the possibility of blistering due to hydrogen trapped inside polymer cavities, because in certain cases, once the component is removed from hydrogen exposure, the blisters can gradually disappear after few days, so it was difficult to make a clear statement.

Apart from linear or scratch abrasion in certain components, mainly generated in the process of disassembling, no clear signs of hydrogen damage were observed on the different parts inspected, except for the valve seat after the 30 mol% H₂ campaign (i.e. 3rd campaign), for which a significant blistering was observed, as shown in Figure 16. It should be noted that blistering was only observed for this component in this campaign and not observed in the 100 mol% H₂ campaign (Figure 17). There is therefore, no clear evidence of the influence of hydrogen on the observed damage, most likely due to a defect in the manufacturing of the component.

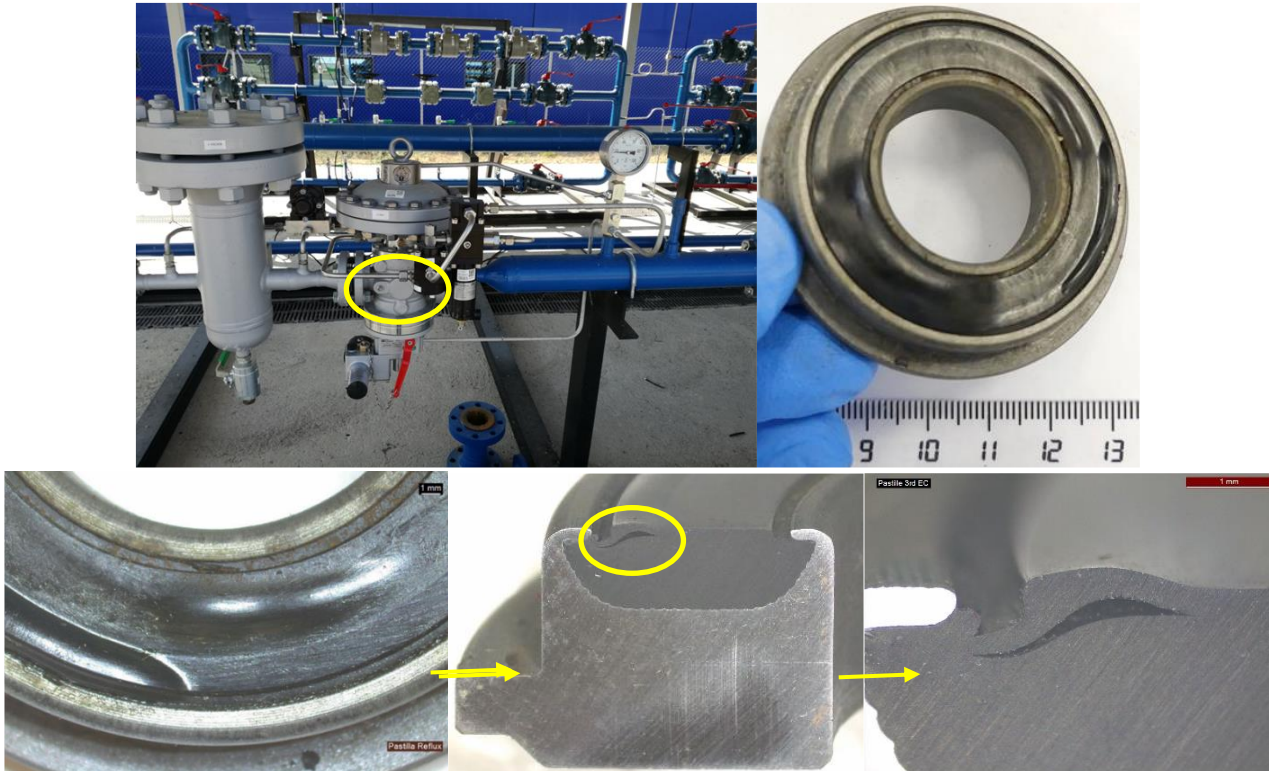


Figure 16. Pressure regulator and details of blistering in valve seat at the conclusion of the 3rd experimental campaign



Figure 17. Valve seats tested at 20% H₂ + impurities of CO₂ and H₂S (left) and 100 mol% H₂ (centre, right). The valve tested at 100 mol% H₂ was cut to verify the absence of blistering or other type of damage

Figure 18 to Figure 22 show the general appearance and some more detailed analysis of some of the examined items. No blistering was observed in the plastic or polymeric components at the time of removal from the testing platform. No cracking was detected for any of the metal components.

At the conclusion of the 100 mol% H₂ campaign, the Elster TRZ2 turbine gas meter was removed from the dynamic section and disassembled for inspection (Figure 23). Except certain accumulation of grease and some dirt in the flow channel (Figure 24), no other signs of damage were observed in the turbine. A detail of the gas meter rotor is given in Figure 25.

D4.4 Final report on systematic validation of testing loop

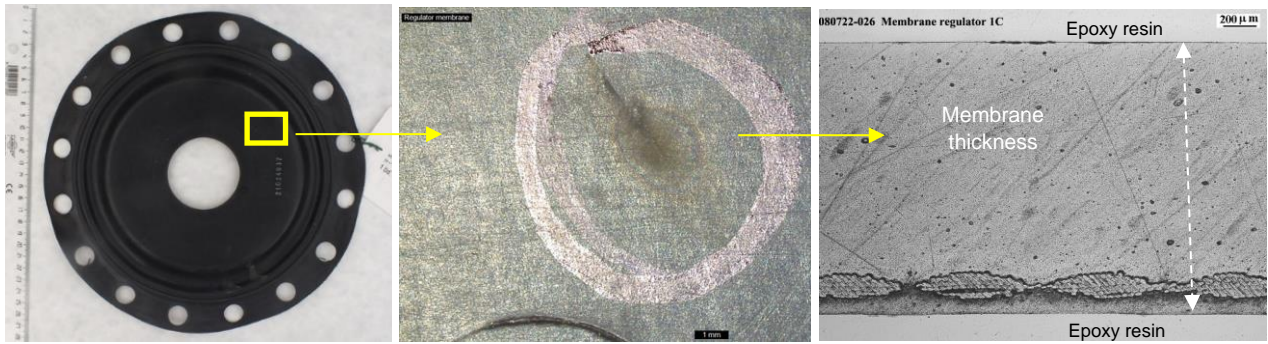


Figure 18. Parts of the pressure regulator after the 20 mol% H₂ exposure: membrane: general appearance (left), detail of area with unknown damaged area (centre) and cross section materialographic probe (right) showing a very superficial damage

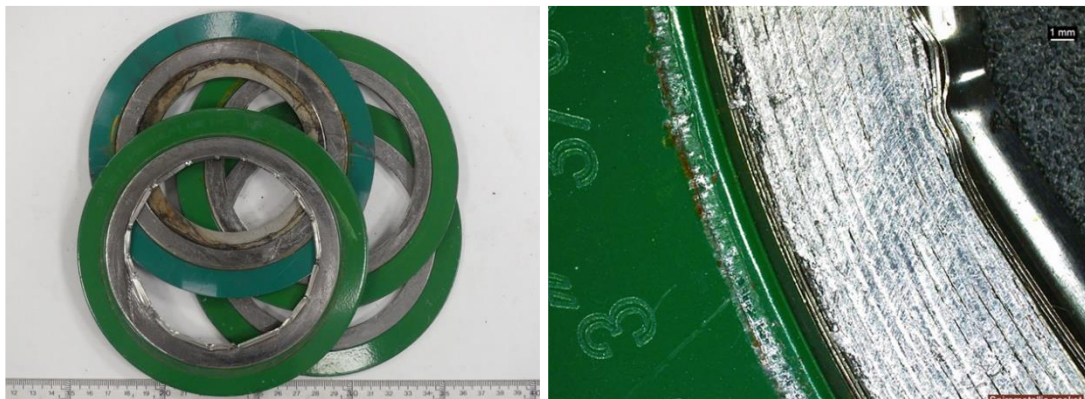


Figure 19. Spirometallic gaskets after the 20 mol% H₂ + of CO₂ and H₂S impurities campaign



Figure 20. Parts of the pressure regulator (left) and detail of O-rings (right) after the 100 mol% H₂ campaign

D4.4 Final report on systematic validation of testing loop



Figure 21. Detail of membrane from the pressure regulator after the 100 mol% H₂ campaign

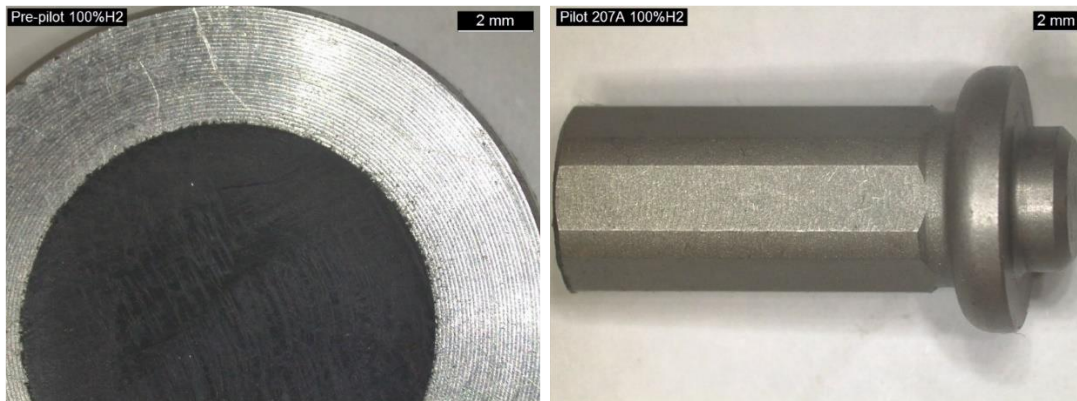


Figure 22. Metallic parts of the pressure regulator after the 100 mol% H₂ campaign



Figure 23. Detail of ELSTER TR22 G100 DN80 Class 600 turbine gas meter after the 100 mol% H₂ campaign



Figure 24. Detail of flow turbine gas meter bodies

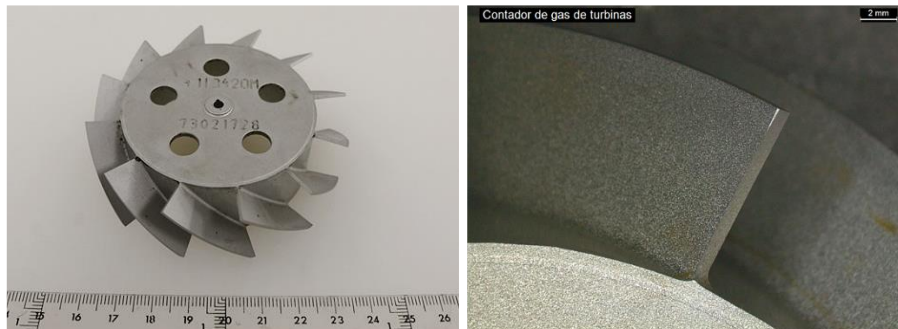


Figure 25. Aluminum gas meter rotor and detail of rotor blade

4.4 Inspection of valves from the static section

The main body of the plug, the ball and the butterfly valves installed in the static section of the R&D platform (Table 2), were disassembled at the conclusion of the four experimental campaigns and inspected to detect signs of hydrogen damage (see details in section 3.3). In general, the Teflon seals did not show any significant damage, except for that which may have been generated in the process of disassembling of the valve. The seal bodies made of Graphoil were, in many cases, broken or fragmented, most probably due to the process of dismantling of the valve, as it is a very soft and flexible material.

Figure 26 to Figure 29 show the general appearance of some of the examined items. It should be noted that, in the two Kurvalf plug valves, one of the two O-rings present a damaged area, with a similar morphology in both rings. The source of this damage is unknown but may be behind the lack of tightness observed in the results from section 4.1.4. Extrusion (nibbling) or over-compression phenomena are coherent with the kind of damage found in the O-rings and can cause such leaks. In any event, this damage is not related to the action of hydrogen gas.

D4.4 Final report on systematic validation of testing loop



Figure 26. Components of the DIDTEK 600-3 valve showing detail of the graphoil and Teflon seals after the 100 mol% H₂ campaign



Figure 27. Components of the ALFA VALVOLE n° 5 (left) and ALFA VALVOLE n° 6 (right) Teflon seals after the 100 %mol H₂ campaign



Figure 28. Components of the KURVALF rose n°2 plug valve and detail of O-ring after the 100 %mol H₂ campaign



Figure 29. Components of the KURVALF red n°1 plug valve showing detail of O-rings after the 100 mol% H₂ campaign

4.4.1 Ball valve analysis (2nd campaign)

As explained in section 4.1.2, a gas leakage was detected in one of the testing ball valves at the end of the 2nd campaign. This failure occurred in a transition between campaigns, after emptying the platform and filling it again at 4 bar with nitrogen. The valve was sent to Tecnia to evaluate the type of damage observed in the valve.

Figure 30 and Figure 31 show details of this screwed ball valve. The visual inspection of the valve prior to its disassembly, revealed a quite significant corrosion in the thread exposed to the air (atmosphere), while the thread in contact to the H₂/CH₄ blend was not corroded, which is logical since the H₂/CH₄ gas mixture is not corrosive. The valve was cut to unscrew the body and closure. A marked not uniform deformation was observed in the Teflon seat located near the closure (Figure 32), being this fact the most likely cause of the leakage observed in the ball valve. It seems that the ball could not be fully aligned with the seat, so the seat was pushed when the valve was closed and deformed by the ball when opened. Therefore, the failure could not be attributed to a hydrogen damage.

A very little abrasive effect was observed in the stainless-steel ball, mainly attributed to the generation of corrosion products from the carbon steel zinc coated body/closure (Figure 33). Corrosion products inside the body of the valve were chemically characterised by energy dispersive x-ray spectroscopy (EDS), using a microanalyser coupled to the SEM (scanning electron microscope). EDS spectra indicated that corrosion products were mainly constituted of zinc (Zn), iron (Fe) and oxygen (O) as zinc and iron oxides.

D4.4 Final report on systematic validation of testing loop

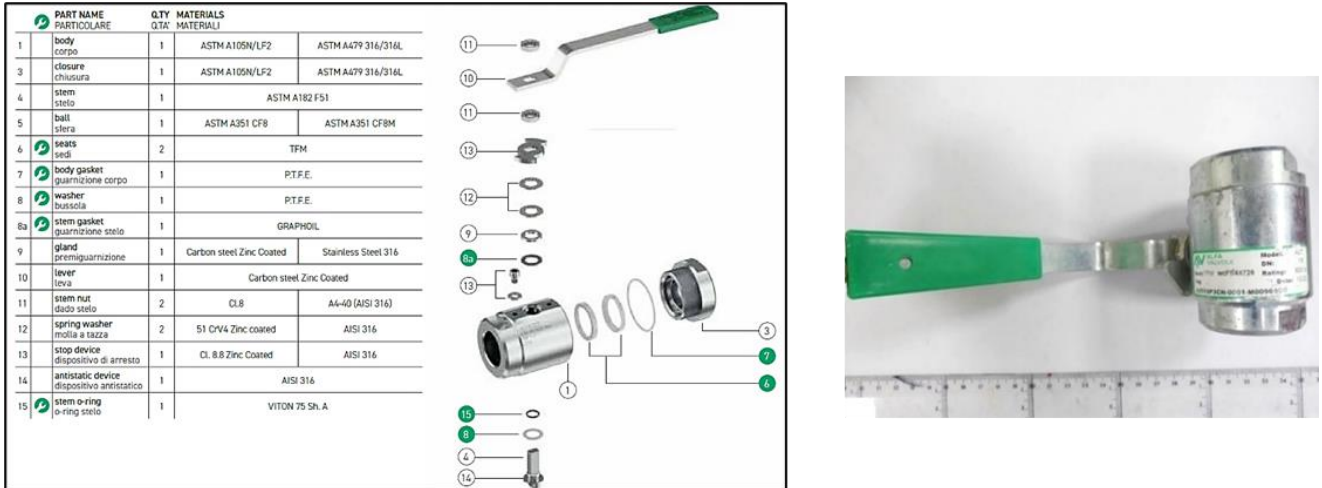


Figure 30. Photograph showing detail of the ball valve sent to TECNALIA (right) and data sheet supplied by the manufacturer (left)



Figure 31. Photographs showing details of the ball valve



Figure 32. Photographs showing detail of the deformed TFM seat

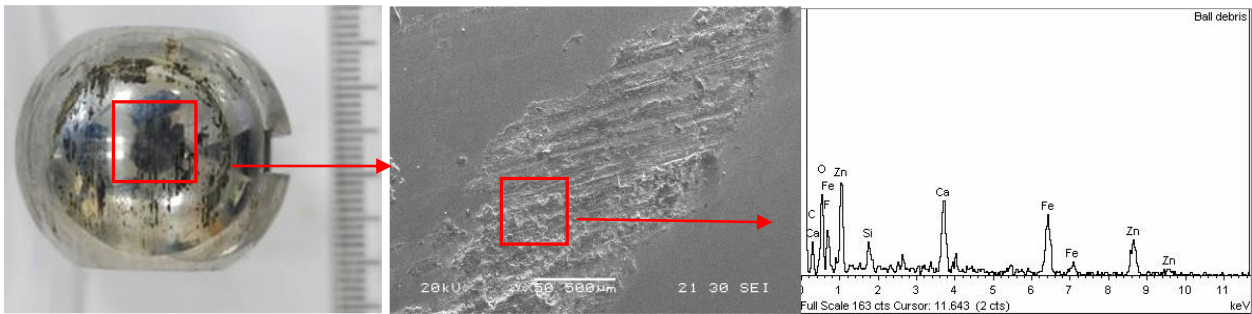


Figure 33. Photograph showing detail of the ball (left) and SEM micrograph of abraded area (centre) with EDS spectrum of this zone (right)

4.5 API 5L steel specimens constant displacement tests

The constant displacement steel specimens were located inside the pig trap, in the loop experimental platform, at FHA and exposed to the different H₂ concentrations. At the conclusion of each experimental campaign, the dynamic section of the loop was depressurised and purged with nitrogen and the pig trap was opened. Figure 34 and Figure 35 show the aspect of the racks with the self-loaded steel specimens inside the pig trap, at the conclusion of the 2nd and 4th experimental campaigns, respectively.



Figure 34. Test specimens inside the pig trap in the loop experimental platform at FHA at the beginning of the 2nd experimental campaign (left) and once concluded (right)



Figure 35. Test specimens inside the pig trap at the conclusion of the 100 mol% H₂ experimental campaign

The results obtained in the constant displacement tests carried out in the four experimental campaigns are detailed below.

4.5.1 C-ring specimens

Table 8 summarises the most significant results obtained in the C-ring tested specimens. After more than 2200 hours of exposure in each experimental campaign, no cracks were found in any of the C-ring tested specimens.

Table 8. Summary of test results for the C-ring tests

Campaign number	Gas composition (80 bar)	Test duration (h)	Steel grade	Condition	Applied stress	Results
1	20 mol% H ₂ 80 mol % CH ₄		X42 base			No cracks
			X52 base			
			X60 base			
2	20 mol% H ₂ 4 mol% CO ₂ 11 ppmv H ₂ S 76 mol % CH ₄		X42 base			No cracks
			X52 base			
			X60 base			
3	30 mol% H ₂ 4 mol% CO ₂ 11 ppmv H ₂ S 66 mol % CH ₄	2200-3000	X42 base	Smooth and notched	100% YS	No cracks
			X52 base			
			X60 base			
4	100 mol% H ₂		X42 base			No cracks
			X52 base			
			X60 base			

C-ring specimens were inspected with a stereo microscope, followed by metallographic sectioning to confirm the absence of cracks, both in the base and notch C-ring samples tested in the four experimental campaigns.

D4.4 Final report on systematic validation of testing loop

The appearance of the tested C-ring specimens after the 100 mol% H₂ experimental campaign is given in Figure 36. Details of the metallographic evaluation are given in Figure 37 and Figure 38.



Figure 36. Detail of tested C-ring specimens after the 100 mol% H₂ campaign

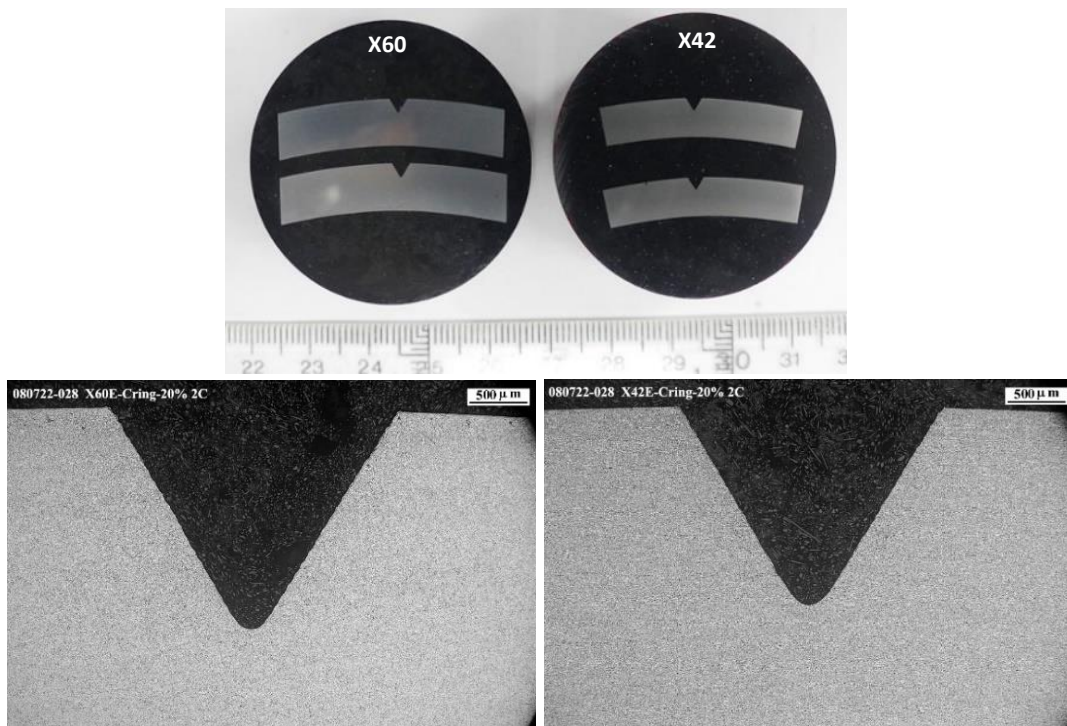


Figure 37. Resin embedded notched C-ring cross sections (up) and optical micrographs from steel grades X60 (down-left) and X42 (down-right) after the 2nd campaign

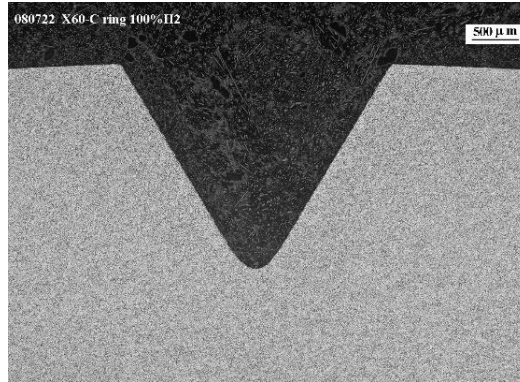


Figure 38. Optical micrograph from notched C-ring cross section of steel grade X60 after the 100 mol% H₂ campaign

Table 9 summarises the most significant results obtained for the 4pb specimens. After more than 2200 hours of exposure in each experimental campaign, no cracks were found in any of the 4pb specimens.

Table 9. Summary of test results for the 4pb tests

Campaign number	Gas composition (80 bar)	Steel grade	Applied stress	Results
1	20 mol% H ₂ 80 mol % CH ₄	X52 base	100% YS	No cracks
		X52 welded		
		X70 base		
		X70 welded		
2	20 mol% H ₂ 4 mol% CO ₂ 11 ppmv H ₂ S 76 mol % CH ₄	X52 base		No cracks
		X52 welded		
		X70 base		
		X70 welded		
3	30 mol% H ₂ 4 mol% CO ₂ 11 ppmv H ₂ S 66 mol % CH ₄	X52 base		No cracks
		X52 welded		
		X70 base		
		X70 welded		
4	100 mol% H ₂	X52 base	No cracks	
		X52 welded		
		X70 base		
		X70 welded		

Figure 39 shows the appearance of welded X70 steel 4pb specimens supported in the loading jig, tested during the 3rd experimental campaign. No cracks were detected during the inspection with a stereo microscope. Metallographic sectioning confirmed the absence of cracks in the base, heat affected zone (HAZ) and weld metal areas both for the specimens tested in the 2nd campaign and for those tested in the 3rd campaign, Figure 40 and Figure 41.

D4.4 Final report on systematic validation of testing loop



Figure 39. Tested X70 base and welded 4pb specimens supported in the loading jig after the 3rd campaign (up) and tested x70 and X52 base and welded specimens after the 100 mol% H₂ campaign

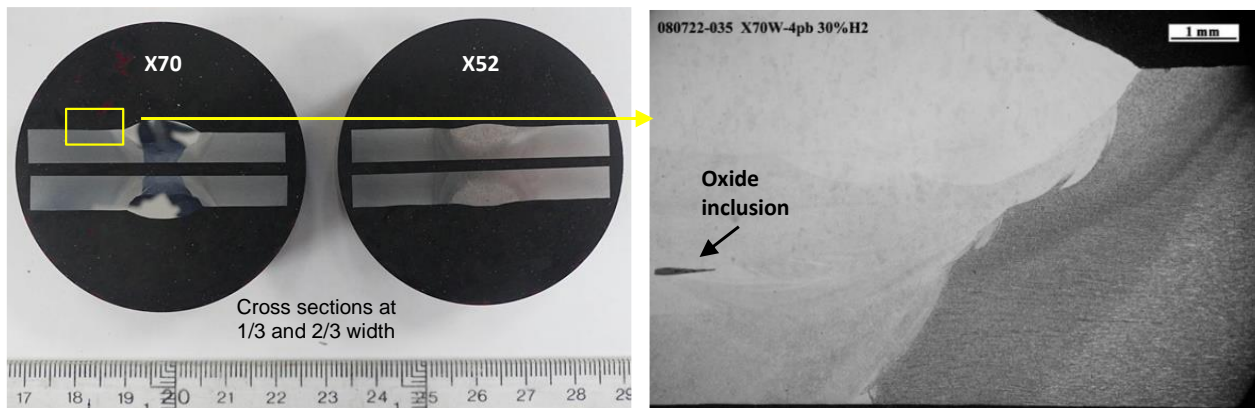


Figure 40. Resin embedded cross sections of 4pb X52 and X70 welded steel specimens (left) and optical micrograph of metallographic section of X70 welded joint (right) after the 3rd campaign



Figure 41. Optical micrograph of metallographic section of X70 welded joint after the 100 mol% H₂ experimental campaign

Figure 42 shows the appearance of the racks with the CT-WOL specimens tested in experimental campaigns 2, 3 and 4. The CT specimens were unloaded (removing the bolt) and then heat tinted (30 min at 300 °C) and broken. The fracture surface was examined by SEM to assess if subcritical cracking occurred from the initial fatigue pre-crack. Measurements of the crack front extent were carried out in three positions and the average crack growth in hydrogen was calculated according to ASTM E1681 standard. No hydrogen crack growth was measured for any CT specimen (crack propagation < 0.25 mm). Fracture surface examination revealed the same fracture mode in the fatigue pre-crack and in the crack front (Figure 43 and Figure 44). The results for these specimens are summarised in Table 10.

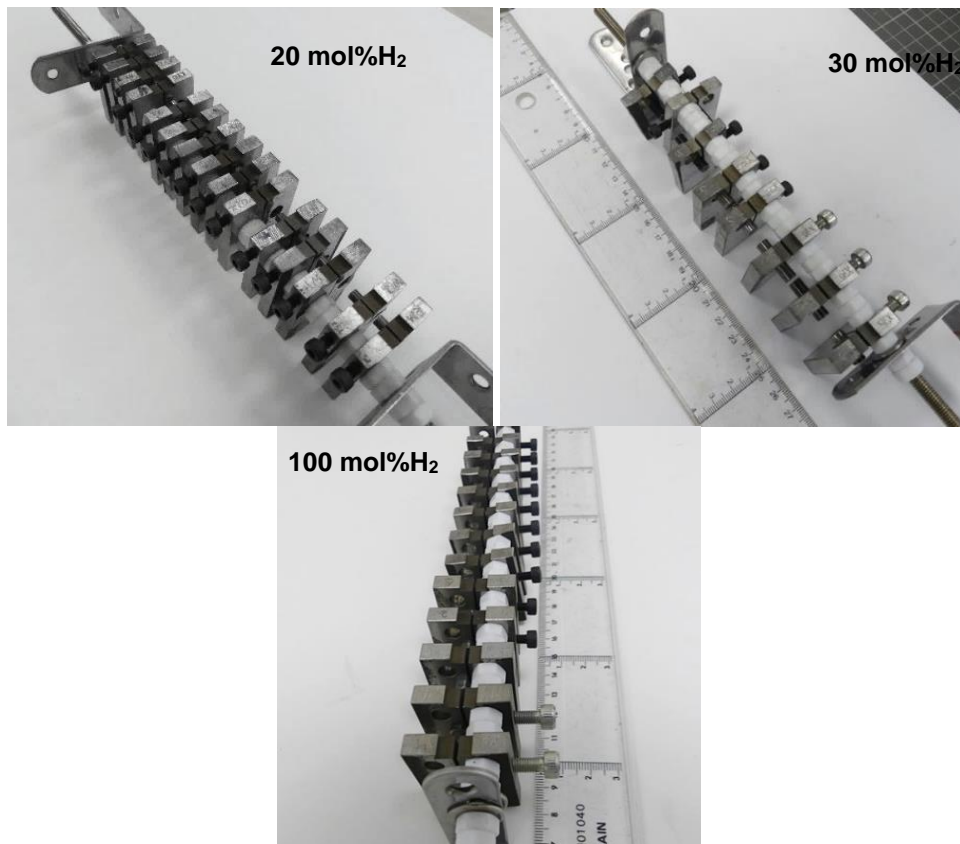


Figure 42. Rack with tested CT bolt loaded specimens in experimental campaigns 2 (top-left) 3 (top-right) and 4 (down)

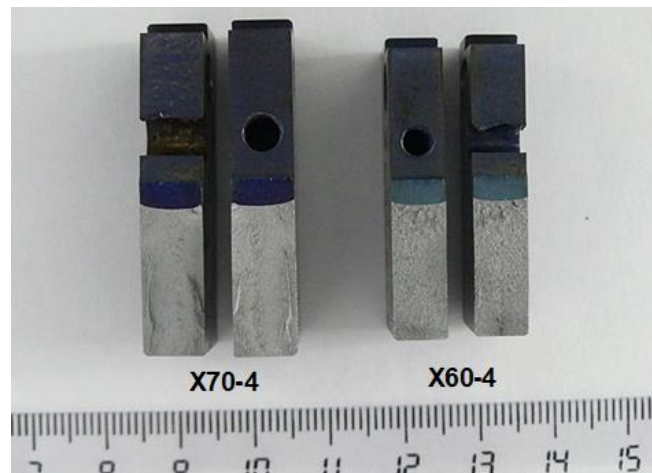


Figure 43. Heat tinted fracture surface of CT-WOL specimens after the 100 mol% H₂ campaign

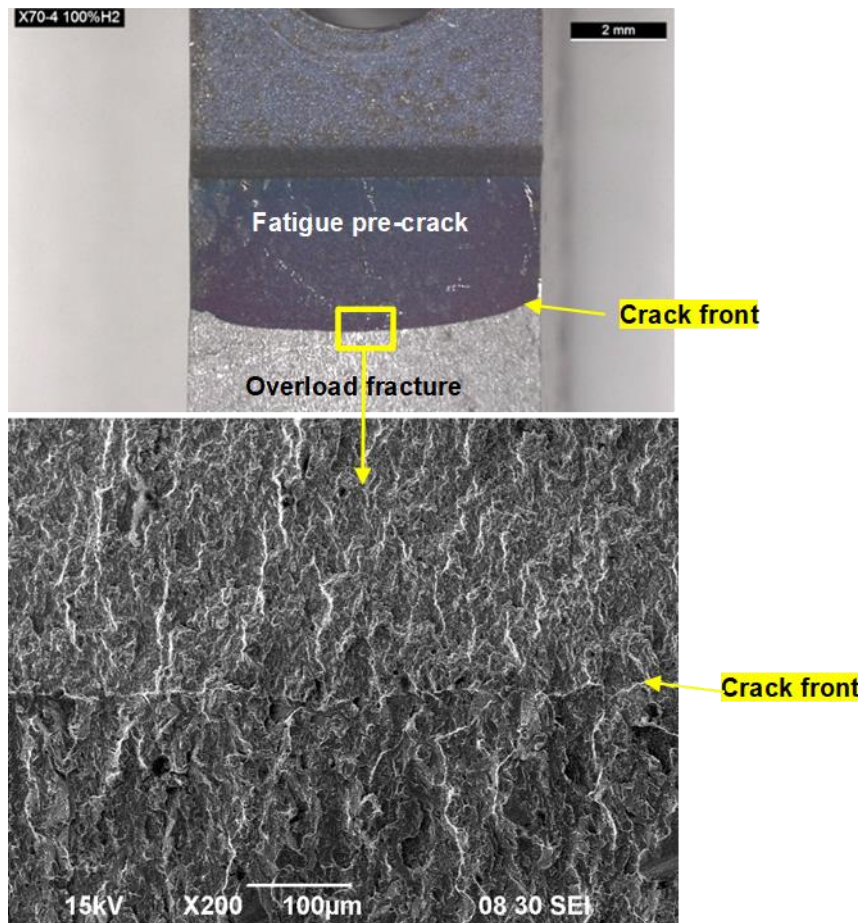


Figure 44. Heat tinted fracture surface of X70 CT-WOL specimens after 100 mol% H₂ exposure and SEM micrograph showing detail of the fatigue pre-crack surface and crack advancing front

Table 10: Summary of test results for the CT-WOL tests

Campaign number	Gas composition (80 bar)	Steel grade	Test duration (hours)	Notch position / orientation	Applied initial stress intensity factor $K_{IAPP}(MPam^{1/2})$	Crack propagation after hydrogen exposure
1	20 mol% H ₂	X52	2200-3000	Base / TL	32	<0.25mm (no crack growth)
	80 mol % CH ₄	X70		Base / TL	41	
2	20 mol% H ₂	X52		Base / TL	32	
	4 mol% CO ₂	X70		Base / TL	41	
	11 ppmv H ₂ S 76 mol % CH ₄	X70 weld		Weld / TL	41	
3	30 mol% H ₂	X60		Base / TL	45	
	4 mol% CO ₂	X70		Base / TL	55	
	11 ppmv H ₂ S 66 mol % CH ₄	X70 weld		Weld / TL	41	
4	100 mol% H ₂	X60		Base / TL	45	
		X70		Base / TL	55	
		X70 weld		Weld / TL	41	

K_{IAPP} =Stress intensity factor applied to the fixed displacement WOL specimen

4.5.2 Welded pipe sections of API 5L pipes

At the conclusion of the 100 mol% H₂ campaign, the welded pipe sections of the API 5L steel pipes were cut and sent to Tecnia for inspection (see section 3.4.2). Figure 45 shows the appearance of the welded pipe sections upon reception in Tecnia. The welded sections were cut again, to limit the inspection area to the welded joint. After visual examination of the internal welded surface, some of the sections were inspected by the magnetic particle testing method.

No accumulation of magnetic particles was observed in the tested welded surfaces, that could indicate the presence of crack-type defects in the samples examined (Figure 46 and Figure 47).

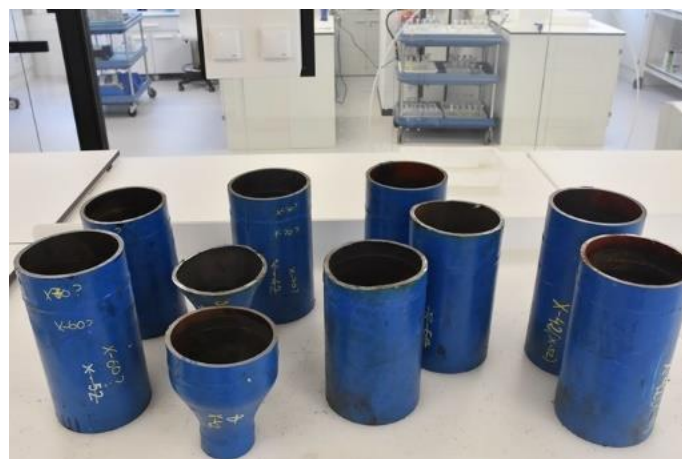


Figure 45. Aspect of the welded pipe sections delivered to Tecnia after the 100 mol% H₂ campaign

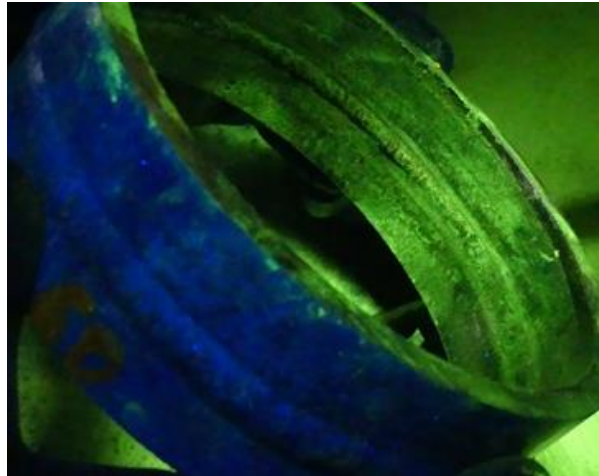


Figure 46. Magnetic particle testing of X42-X52 welded joint



Figure 47. Magnetic particle testing of X52-X60 welded joint

5 Slow Strain Rate Tests

Table 11 summarises the results obtained in the SSRT carried out in the steels grades X52, X60 and X70.

Table 11. Summary of the results obtained in the SSR tests

Steel grade	Test environment	Displacement rate (mm/s)	RA (%)	RA ratio	NTS (MPa)	NTS ratio	YS (MPa)	Fracture mechanisms
X52	Air	5x10 ⁻⁵	28.62		758		710	Dimples
X52	80 bar H ₂	5x10 ⁻⁵	11.54	0.40	731	0.96	724	Dimples + cleavage
X60	Air	5x10 ⁻⁵	29.04		979		924	Dimples
X60	80 bar H ₂	5x10 ⁻⁵	9.71	0.33	903	0.92	903	Dimples + cleavage
X70	Air	5x10 ⁻⁵	22.27	-	1069		972	Dimples
X70	80 bar H ₂	5x10 ⁻⁵	9.37	0.42	965	0.90	958	Dimples + cleavage

H₂ purity: 99.999

A quite significant reduction of area (RA) loss and therefore, loss of ductility, is measured in all the notched steel specimens when tested in H₂ gas at 80 bar. It is important to say that the RA loss in notched specimens is higher than the one measured from smooth specimens. In any case, the notched tensile strength (NTS), which is the key parameter when performing material screening tests with notched specimens, is barely reduced due to hydrogen, with NTS ratios equal to or greater than 0.90. In general, and in a qualitatively way, NTS ratios comprised between 0.90 and 0.96 are associated with a small category / low index of embrittlement.

Small differences are observed when comparing X52, X60 and X70 steel specimens. The higher loss of ductility is observed for the bainite X60 steel. The lower NTS ratio, this is, the higher embrittlement effect, is observed in the steel with higher mechanical resistance (X70).

The fracture surface of the tested notched specimens was analysed using the SEM. The fracture surface of the specimens tested in air was fully ductile, Figure 49, with dimples (microvoid coalescence) formation. For all the specimens tested in hydrogen, two zones were observed: a fully ductile central region and a peripheral region with transgranular brittle cleavage, with no evidence of dimples, Figure 50, Figure 51 and Figure 52. As it can be seen in Figure 52, the brittle fracture zones of the X70 steel specimens tested in H₂, show certain secondary crack penetration.

D4.4 Final report on systematic validation of testing loop

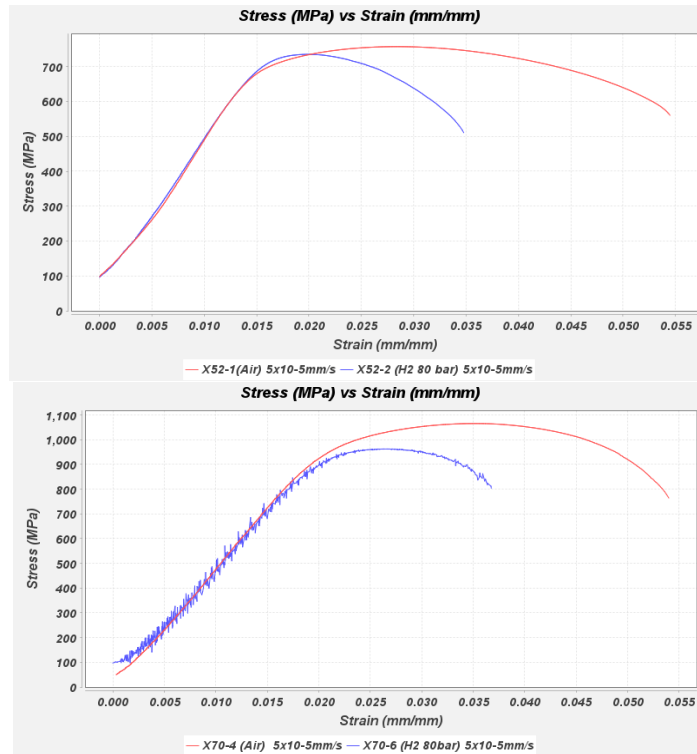


Figure 48. Stress strain curves of notched SSRT specimens tested in air and in H₂ (80 bar)

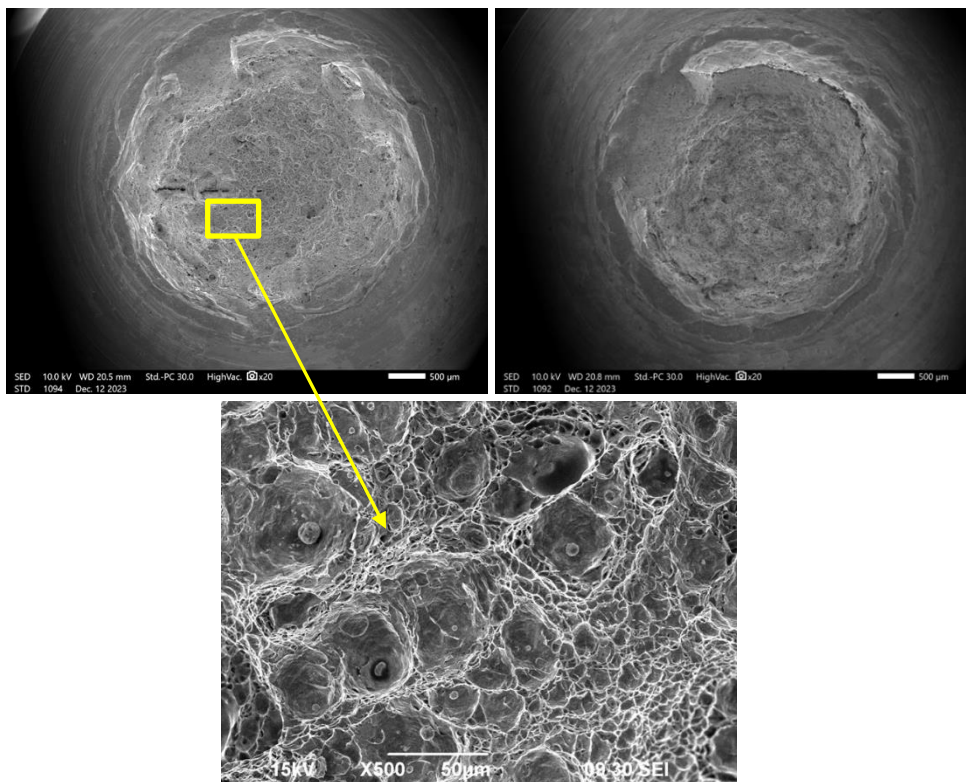


Figure 49. Electron micrographs showing fully ductile fracture surface of SSRT specimens tested in air: X52 (up-left), X60 (up-right). Numerous particles within the dimples are observed (down)

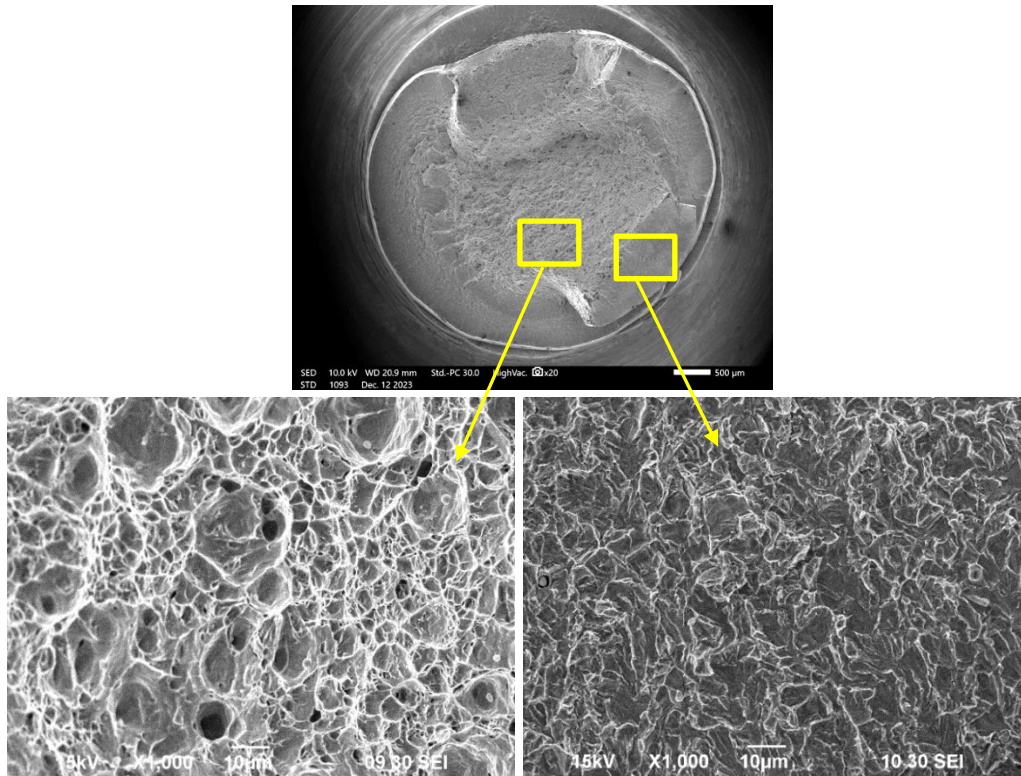


Figure 50. Electron micrographs of fracture surface of X52 SSRT specimen tested in H₂ at 80 bar, showing a central region with dimples generation (down-left) and a peripheral region with transgranular cleavage (down-right)

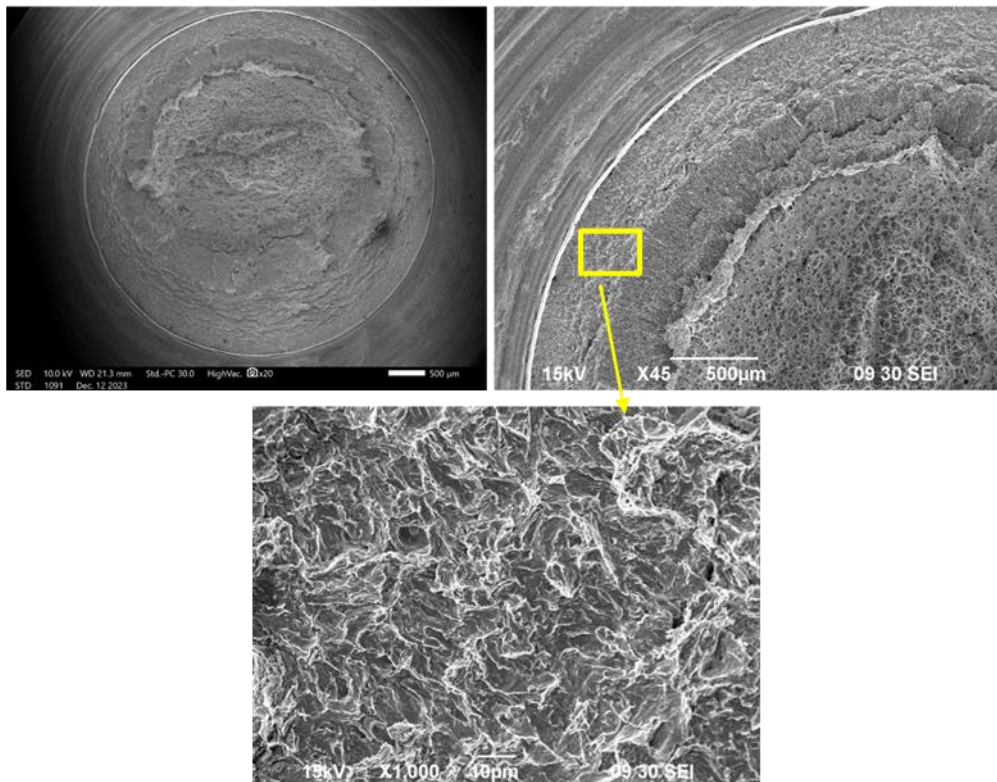


Figure 51. Electron micrographs of fracture surface of X60 SSRT specimen tested in H₂ at 80 bar (up) and detail of the peripheral region with transgranular cleavage (down)

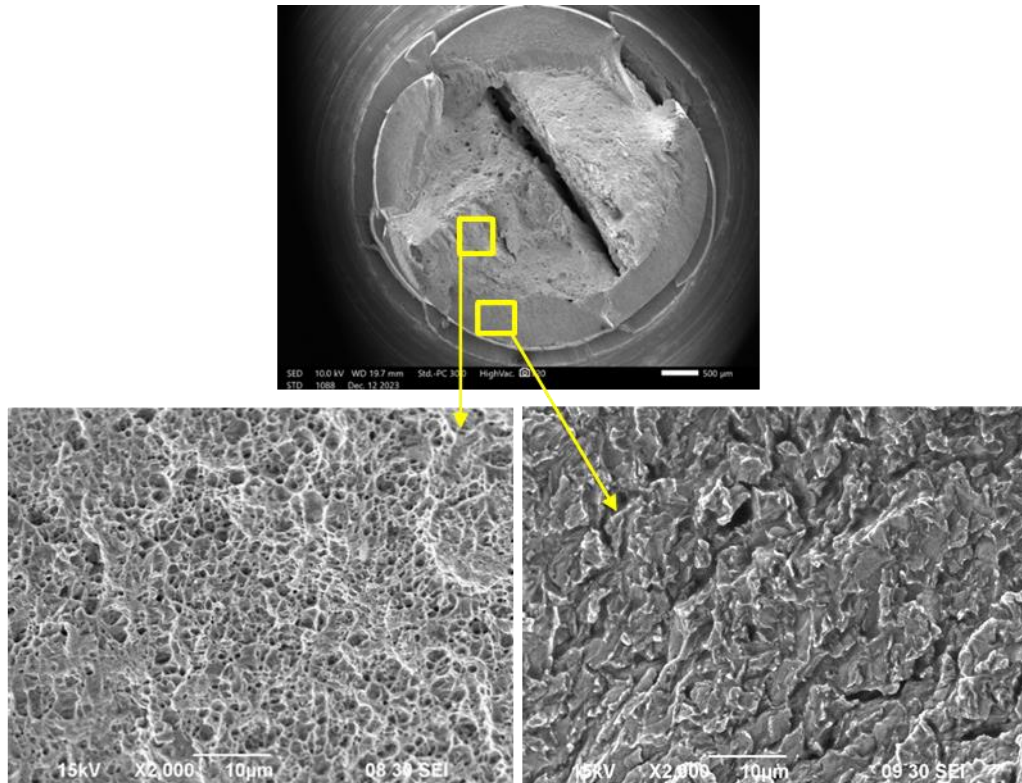


Figure 52. Electron micrographs showing fracture surface of X70 SSRT specimen tested in H₂ at 80 bar (left) and detail of the peripheral region with transgranular cleavage and secondary crack penetration

The classification of embrittlement categories (HEE index) based on the NTS ratio is given in the document from NASA “*Hydrogen embrittlement*” [14]. It is important to say that this is a qualitative classification and for components design it should be combined with fracture analysis. As additional information, it should be noted that the Canadian standard ANSI/CSA-CHM [15] “*Test methods for evaluating material compatibility in compressed hydrogen applications*” (2018), indicates that NTS ratios below 0.5, automatically discard carbon steel for service in hydrogen. For ratios higher than 0.5, the standard proposes to perform fatigue or fracture toughness tests to qualify the material. The qualification of the material is performed on three heats of the material, considering both the base material, the HAZ and the welded material.

6 Conclusions

The tolerance towards hydrogen of the API 5L steels grades X42, X52, X60 and X70, valves and equipment installed in the HIGGS' R&D platform built at FHA, has been evaluated for the operating conditions established in the four experimental campaigns carried out in HIGGS.

The most relevant conclusions reached within the framework of the HIGGS project are presented below.

- One of the key aspects of the HIGGS project has been the development of an experimental test platform that reproduces on a small scale the components and materials in a typical natural gas high-pressure network.
- On the whole, all the testing valves remained tight for the duration of the test regardless the hydrogen content in the pipe, with just minor hydrogen losses due to hydrogen leakage through the body of the valves.
- The significant leakages detected in the 2nd experimental campaign (i.e. 20 mol% H₂ with trace impurities of H₂S and CO₂) in the line containing flanged valves is related to incorrect reassembly of the valves disassembled after the 1st experimental campaign. It is therefore concluded that reassembly of the valves should be done by the manufacturer expertise.
- Under 100 mol% H₂ service, the pressure oscillations in the line are higher than those in previous test with hydrogen blends, but it remains in any event low enough to discard a potential leak.
- The internal tightness of flanged valves has also been assessed towards 100 mol% hydrogen service. The suitability of plug valves must be however further assessed with complementary tests.
- The analysis of the ball valve with a leakage at the end of the 2nd campaign (i.e. 20 mol% H₂ with trace impurities of H₂S and CO₂) was due to a clear misalignment between the ball of the valve and the Teflon seat, and not to hydrogen damage.
- The results of the inspection carried out in the valves, pressure regulator, cartridge filter and turbine gas meter components after their exposure to the different hydrogen mixtures, showed no apparent damage on the different parts examined. Only, in the 30 mol% H₂ campaign, it was observed a significant blistering in a valve seat from the pressure regulator. This blistering was not detected however in the 100 mol% H₂ level. It cannot therefore be established clear evidence of the influence of hydrogen, and most likely due to a defect in the manufacture of this component.
- The Pd-based double skinned membrane prototype showed a great gas separation performance. The long-term stability experiment of Membrane #1 led to a good gas separation performance, where the prototype showed a stable permeate flow during the 500h operation with a hydrogen purity over 96 mol%. In the case of Membrane #2, feed flow and feed pressure were tuned to obtain the maximum hydrogen recovery possible, reaching 90 mol% at 80 bar feed pressure and 6.15 NI·min⁻¹ feed flow with the lowest H₂ content in the retentate of 2.7 mol%, and H₂ purities in the permeate higher than 99.5 mol% after 175h operation. These results show that the membrane technology is promising for the H₂ recovery and purification of low H₂-concentrated gas streams. The membrane prototype should be developed and validated at a larger scale (higher volume to be treated), longer times and with real gas mixtures (impurities, odorants, etc).

D4.4 Final report on systematic validation of testing loop

- The magnetic particle inspection method carried out in the welded pipe sections of the API5L steels located in the R&D platform, did not show discontinuities such as cracks or pits, after the approximately 11000 hours of exposition to the different hydrogen concentrations of the four experimental campaigns.
- No cracking was detected for any of the constant displacement specimens type C-ring and 4pb, neither in the base material, the HAZ, nor the welded material, stressed at 100% of the materials yield strength, and exposed to the different H₂ blends, at 80 bar pressure, and tests duration up to 3000 hours. No crack propagation could be also noticed in CT-WOL specimens either. It can be therefore concluded that, in the tests to evaluate the compatibility of the steels using constant deformation specimens, no signs of embrittlement were detected after the four experimental campaigns carried out.
- The results of the SSRT tests carried out in air as reference medium and in 100 mol% H₂ at 80 bar pressure, yielded values of the NTS ratio comprised between 0.90 and 0.96. These ratios are categorized as low sensitivity to hydrogen embrittlement. It was observed however a quite significant loss of ductility in the notch specimens mainly manifested in the loss in the RA values as well as in the morphology of the fracture surface. Whereas a fully ductile fracture surface was observed in the specimens tested in air with dimples generations, areas of transgranular cleavage were detected on the periphery of the specimens tested in hydrogen.
- Depending on the loading conditions -static or rising load- and the presence or absence of notches in the material, the degree of embrittlement could be different. In general, rising load tests produce higher embrittlement indexes in the material. Constant displacement tests that allow the exposition of samples significantly longer test times, should be combined with rising load tests: SSRT, fracture toughness and fatigue, especially for steel qualification or component design.
- Finally, it can be concluded that the results obtained both in the constant displacement tests carried out in the R&D testing platform and in the SSRT, are indicative of low susceptibility to hydrogen embrittlement for the API 5L steels grades X42, X52, X60 and X70, in the tests conditions established in HIGGS. Besides, when damage was found in the different components of the testing valves or equipment it could not be assigned to the effect of hydrogen gas.
- According to the tests performed in HIGGS, the high-pressure natural gas grid seems ready for the transport of hydrogen at blending levels until reaching 100 mol% concentration. With respect to the steel pipes, although the results obtained in the mechanical tests of the four API 5L steels under study indicate a low hydrogen embrittlement susceptibility, additional fracture toughness research should be performed to achieve a proper material certification.

Bibliography and References

- [1] A. Arratibel, A. Pacheco Tanaka, I. Laso, M.van Sint Annaland, F. Gallucci. Development of Pd-based double-skinned membranes for hydrogen production in fluidized bed membrane reactors, *Journal of membrane science*, Volume 550, 15 March 2018, Pages 536-544
- [2] API 5L, Specification for line pipe (2020)
- [3] ISO 7539-5, Corrosion of metals and alloys. Stress corrosion testing. Part 5: Preparation and use of C-ring specimens (1996)
- [4] ASTM G38, Standard practice for making and using C-Ring stress-corrosion test specimens (2021)
- [5] ISO 7539-2, Corrosion of metals and alloys. Stress corrosion testing. Part 2: Preparation and use of bent-beam specimens (1996)
- [6] ASTM G39, Standard practice for preparation and use of bent-beam stress-corrosion test specimens (2021)
- [7] ASTM E1681, Standard test method for determining threshold stress intensity factor for environment assisted cracking of metallic materials (2020)
- [8] ISO 7539-6, Corrosion of metals and alloys. Stress corrosion testing. Part 6: Preparation and use of precracked specimens for tests under constant load or constant displacement (2020)
- [9] ASME B31.12, Hydrogen piping and pipelines (2019)
- [10] ISO 17638, Non-destructive testing of welds. Magnetic particle testing (2016)
- [11] ASTM G142, Standard test method for determination of susceptibility of metals to embrittlement in hydrogen containing environments at high pressure, high temperature, or both (2022)
- [12] ASTM G129, Standard practice for Slow Strain Rate Testing to evaluate the susceptibility of metallic materials to environmentally assisted cracking (2021)
- [13] ISO 7539-7, Corrosion of metals and alloys. Stress corrosion testing. Part 7: method for slow strain rate testing (2005)
- [14] NASA, Hydrogen embrittlement (2016)
- [15] ANSI/CSA-CHM, Test methods for evaluating material compatibility in compressed hydrogen applications (2018)

Acknowledgements

This project has received funding from the Fuel Cells and Hydrogen 2 Joint Undertaking (now Clean Hydrogen Partnership) under Grant Agreement No. 875091 'HIGGS'. This Joint Undertaking receives support from the European Union's Horizon 2020 Research and Innovation program, Hydrogen Europe and Hydrogen Europe Research.

